10419
NACA TN 4085

TECH LIBRARY KAFB, NM
0066956

NATIONAL ADVISORY COMMITTEE FOR AERONAUTICS

TECHNICAL NOTE 4085

METHOD OF SPLIT RIGIDITIES AND ITS APPLICATION TO VARIOUS BUCKLING PROBLEMS

By P. P. Bijlaard

Cornell University

Washington
July 1958

AFMDC
TECHNICAL LIBRARY
AFL 2811

TECH LIBRARY KAFB, NM
0066956

NATIONAL ADVISORY COMMITTEE FOR AERONAUTI(

TECHNICAL NOTE 4085

METHOD OF SPLIT RIGIDITIES AND ITS APPLICATION TO VARIOUS BUCKLING PROBLEMS

By P. P. Bijlaard

SUMMARY

A comprehensive treatise on the method of split rigidities is presented. First the principles upon which the method is based are discussed. It is shown on new examples how these principles are applied. These applications are divided into problems where all component modes into which the actual behavior of a composite structure is split have the same boundary conditions and into those where these boundary conditions differ. Examples of the first type include sandwich columns with various boundary conditions, columns with batten plates, and latticed columns; examples of elastic and plastic buckling of sandwich plates with orthotropic core and of corrugated-core sandwich plates are also given. This type includes problems based on the same principles where only one mode has to be considered. As an example, the buckling stress of homogeneous plates under nonhomogeneous stresses in their plane is expressed in terms of their critical stress under homogeneous compression. To this group also belongs the determination of the ultimate load of plates under compression. An explicit formula is derived for the buckling stress of stringer panels which is a new example of the second type of problem. The problems were chosen so that the correctness of the method, which is basically an approximate one, can be shown by comparison with exact calculations or tests.

INTRODUCTION

In several papers a method has been used for calculating the buckling stresses of structures that buckle in composite modes which is called the "method of split rigidities." The method consists of splitting the buckling deflection into two or more component modes and expressing the buckling stress in terms of the critical loads for these component modes. References 1 to 19 are based partly or completely on this method.

For example, in a sandwich plate (refs. 5, 9, 11, 12, and 14) there are three different buckling modes: (1) That of the single faces,

(2) that of the complete sandwich plate, assuming the faces to have zero flexural rigidity but assuming the core to have infinite shear rigidity, and (3) that of the complete sandwich plate, assuming the faces to have zero flexural rigidity and assuming the faces to be infinitely rigid against extension. In the case of a T-section (ref. 13) the three modes are: (1) Bending about the Y-axis situated in the plane of the web, (2) twisting about the shear center axis, and (3) plate buckling. In the case of buckling by general instability of a long cylindrical shell with stiffening rings under external pressure (ref. 19) the component modes are buckling as an orthotropic shell, assuming the rigidity of the rings to be uniformly distributed along the length of the shell, and buckling of the shell between the rings. In the case of stringer panels (ref. 18) practically exact solutions are obtained by this method for conventional panel buckling as well as for forced crippling (refs. 16, 18, and 20).

Formulas for buckling loads or stresses have been derived in earlier papers and new ones will be presented herein by establishing equations between external and internal actions. In references 1, 2, 3, and 6 the external and internal actions considered were the external and internal bending moments. In references 7 and 13 bending as well as torsional moments were considered. Bending moments in a cross section as well as deflecting and restraining transverse forces acting on an element were considered in references 4, 9, 11, 13, and 16. The actions and reactions considered in references 14, 15, 17, and 19 were the amounts of work done by deflecting and restraining forces. Columns and plates with initial deflections were considered in a footnote of reference 1 and in reference 15.

The method of split rigidities was also applied in the postbuckling range (refs. 15 and 17). It is very powerful and leads to simple results in cases where a solution by existing methods is practically impossible. It was successfully used in two other projects (refs. 13 and 17). Until the present only a few other investigators have used this method (refs. 21, 22, and 23) probably because no general comprehensive treatise on it has yet been made available. Therefore the purpose of the present report is to give such a general explanation, with examples of the method of application in various special cases.

The present investigation was carried out at Cornell University under the sponsorship and with the financial assistance of the National Advisory Committee for Aeronautics. The examples dealing with the ultimate load of plates under compression and with buckling of stringer panels are part of earlier work done for the Bell Aircraft Corporation. The author wishes to express his appreciation for the valuable cooperation of all concerned and to the Bell Aircraft Corporation for its permission to publish the abovementioned examples.

SYMBOLS

A	total cross section of column
A,B,D,F	plastic reduction coefficients for plastic buckling of plates
A_d	cross section of diagonal
A_{st}	cross section of stiffener
A_v	cross section of vertical
a	half wave length of buckling for plate
b	width of plate; also, width of bay of stringer panel
b_e	effective width of plate
C	constant; also spring constant (foundation modulus)
c	center-to-center spacing of batten plates in built-up column; also, free length of single struts in latticed column
c_o	effective free length of single struts between batten plates
D	deflecting force
D_{Q_x}, D_{Q_y}	ratios of shear to shear angle
E	elastic modulus
E_c	elastic modulus of corrugation
E_s	elastic modulus of faces (skin) in sandwich plate; also, secant modulus in section "Ultimate Load of Plates Under Compression"
E_t	tangent modulus
E_{tc}	tangent modulus of corrugation
G_c	modulus of rigidity of sandwich core

G_x, G_y	moduli of rigidity in X- and Y-directions of sandwich core
H	total thickness of sandwich column or sandwich plate, $t + 2h$
h	center-to-center distance of single struts of built-up column; also, thickness of single face of sandwich column or sandwich plate
I	moment of inertia
I_c	moment of inertia of single strut of built-up column
I_f	moment of inertia of single face of sandwich plate
I_r	moment of inertia of reduced built-up column, $Ah^2/4$
I_s	moment of inertia of reduced sandwich column or sandwich plate, $(1/2)h(t + h)^2$
K	constant
k	buckling stress coefficient defined by equation (142)
k_0, k_1, k_2	buckling stress coefficients referring to cases 0, 1, and 2, respectively
k_s	buckling stress coefficient defined by equation (145)
$k_{1m}, k_{2m}, \ldots$	coefficients in equation (104)
L	effective length of column
l	length of column; also, length of stringer panel
l_r/r	effective slenderness ratio for reduced case of built-up column
l_{eq}/r	effective slenderness ratio of built-up column
M	moment
M_x, M_y	bending moments
M_{xy}, M_{yx}	torsional moments

$m = \left(l_{eq}/r\right)/\left(c/r_c\right)$

N	flexural rigidity of homogeneous plate; also, flexural rigidity of face of sandwich plate
N_s	flexural rigidity of reduced sandwich plate, given by equation (59)
$n = l/c$	
n'	number of bays of stringer panel
P	buckling load
p,q	coefficients in equations (108) and (203)
Q	shear force; also, transverse shear force in plate
Q'	transverse shear force that would cause a unit angular distortion in latticed column
R	restraining force
r	radius of gyration of reduced built-up column, h/2; $r = r_x = r_y$ if $r_x = r_y$
r_c	radius of gyration of single strut of built-up column
r_x, r_y	ratios defined by equations (78) and (81)
$\bar{r}_x, \bar{r}_y$	ratios defined by equations (120) and (123)
S	spring
S, S^{II}, S^{IV}	quarter spring constants for plates
t	core thickness of sandwich column or sandwich plate; also, thickness of homogeneous plate
u_m	normal function
v	translation of single struts per unit shear force in batten plates
w	deflection

x,y,z	coordinates
X,Y	directions
Y	function of y only
α	angle
α_1,α_2	coefficients defined by equation (A6)
α_m	coefficient in equation (102)
β	factor in equation (35)
Γ	aspect ratio of buckle in buckled plate, a/b
γ	angular distortion; also, ratio defined by equation (221)
δ	elongation
ϵ	strain
ϵ_m	membrane strain
ζ	value $\ll 1$ in equation (228)
η	reduction factor for plasticity for concentric buckling of plates
$\bar{\eta}$	reduction factor for plasticity for finite deflection of plates
θ	angle; $\theta = \theta_x = \theta_y$ if $\theta_x = \theta_y$
θ_x,θ_y	ratios defined by equation (73)
κ	ratio defined by equation (226) for stringer panel
$\lambda = \pi/a$	
μ	ratio defined by equation (95)
ν	Poisson's ratio
ξ	slope of column in case 2 of latticed column
σ	normal stress

σ_e	normal stress at edge
σ_m	membrane normal stress
σ_z	normal stress in plane parallel to middle plane of sandwich plate
τ	coefficient in equations (151) and (154)
$\Phi(x,y)$	function of x and y
φ	ratio defined by equation (211)
ψ	defined by equation (212)
Ω	ratio defined by equation (225) for stringer panels

Subscripts:

a	actual (fig. 10(b))
b	bending
cr	critical
e	external
eq	equivalent
h	homogeneous
i	internal
m	maximum
mid	center (middle)
p	postbuckling; also, refers to fictitious end deflections as shown in figure 10(b)
r	reduced case
s	skin (face) for sandwich plate; also, secant in section "Ultimate Load of Plates Under Compression"
st	stiffener
u	uniform
ult	ultimate

x,y refer to X- and Y-directions, respectively; also, refer to X- and Y-strips, respectively, for orthotropic sandwich plate

ys yield stress

0,1,2,...n refer to cases 0, 1, 2, . . . n, respectively

DESCRIPTION OF METHOD

The method of split rigidities as applied to buckling problems may be described as follows:

(1) Splitting into two or more component cases: The elastic or elastoplastic behavior of a composite structure is split into two or more component cases for which the individual buckling stresses can be easily determined. For example, the deflection w of a sandwich plate with membrane faces is split into its deflections w_1 from bending alone (case 1) and w_2 from shear deformation alone (case 2). It is assumed that in the composite structure the component buckling deflections w_1 and w_2 have the same shape as in cases 1 and 2 where they occur alone. The accuracy of the method will be greater the better this assumption is fulfilled. If it is exactly fulfilled, which as explained in this report is only possible if w_1 and w_2 have the same shape, the method is exact.

(2) External actions and internal reactions: With the shapes of the component deflections for the combined case thus determined, it is always possible to establish equations between the external actions and the internal reactions. These actions and reactions may be the external and internal moments acting in a cross section, the deflecting and restraining forces acting upon a small element, or the work done by deflecting and restraining forces.

(3) External action: If the actual combined case is split into two or more, say n, component cases with deflections w_1, w_2, w_3, . . . w_n, the external action is proportional to the actual buckling load P_{cr} for the combined case and may be expressed in terms of P_{cr} and the individual deflections w_1, w_2, w_3, . . . w_n. For example, splitting the deflection w of a sandwich column with membrane faces into the deflection w_1 from bending and the deflection w_2 from shear deformation, the external moment M_e for the combined case is equal to $P_{cr}(w_1 + w_2)$.

(4) Internal action: As stated under item (1), in the combined case with a deflection $w = w_1 + w_2$, the component deflections w_1 and w_2 are assumed to have the same shapes as in the separate cases 1 and 2 with buckling loads P_1 and P_2. The internal reactions depend only on the shape of the deflection and not on the magnitude of the compressive force. Therefore, the internal reactions in the combined case are equal to those in case 1 alone since additional deformations (case 2) increase the deflections but not the internal reactions. In the same way it follows that the internal reactions are equal to those from case 2. For example, in a sandwich column with membrane faces, the deflection w_2 from shear deformation increases the deflection beyond w_1 from bending, but it does not increase the internal moment from w_1, and vice versa, as shown extensively in reference 11.

As will be explained later, the rigidities of the structure against the partial deflections w_1 and w_2 can be considered to be supplied by sets of springs S_1 and S_2 with different spring constants C_1 and C_2 acting in series to restrain the deflection of a column without any proper flexural rigidity (fig. 1). Hence it is obvious that the internal reaction for the combined case, that is, of the combined springs, is equal to that of the separate springs S_1 or S_2.

(5) Problems where component cases are coupled: The statements under item (4) are true only if the deformations for cases 1 and 2 can occur independently without restraining each other, such as the bending and shear deformation of a sandwich column with membrane faces. If this is not so, for example, if the faces have their own proper flexural rigidity, the internal action is increased above that from case 1 or case 2 alone. This can be taken into account in several ways. If the coupling occurs externally by a third agency, such as in the above example, this coupling case (case 0) can be first ignored; that is, the proper flexural rigidity of the faces is assumed to be zero. Finally the axial restraint offered by this coupling rigidity is added to the buckling load of the remaining system. This was done, for example, in reference 11. If cases 1 and 2 themselves are coupled, that is, if they are coupled internally (so that a deformation from case 2 adds to the internal reaction from case 1 and vice versa) as occurs, for example, in reference 13, the extra restraint offered by case 2 is simply added to the internal action from case 1 and vice versa. Also a combination of these methods can be used.

(6) Expression of internal actions and hence of buckling load in terms of buckling loads for component cases: The internal action for case 1 due to a deflection w_1 is equal to the external action for that case, if it occurs separately, which is proportional to the buckling

load P_1 for that case and can be expressed in terms of P_1 and w_1. For example, for case 1 of the sandwich column considered in the section "Introduction," the internal moment M_{i1} from case 1 is equal to the external moment $P_1 w_1$. According to item (4) this is also the internal moment M_i for the combined case. Hence from item (3) the equation of external and internal moment for the combined case leads to the equation $P_{cr}(w_1 + w_2) = P_1 w_1$. Similarly, the internal moment for the combined case is equal to that for case 2, which is again equal to the external moment for that case, giving $M_i = P_2 w_2$. Equating this internal moment to the external moment gives $P_{cr}(w_1 + w_2) = P_2 w_2$. Elimination of w_1 and w_2 gives P_{cr} in terms of P_1 and P_2. If the component cases are coupled and the latter method under item (5) is used, as will usually be done in problems where cases 1 and 2 have different boundary conditions, the internal action will contain both partial deflections w_1 and w_2. Further, in such problems the external action is usually expressed as $P_{cr}(w_1 + \varphi w_2)$ or $P_{cr}(w_2 + \gamma w_1)$ where φ and γ differ from 1, so that after elimination of w_1 and w_2 a more complicated formula for P_{cr} in terms of P_1 and P_2 results than for problems where cases 1 and 2 have the same boundary conditions.

If splitting into three different cases is necessary the same method is used, equating the external actions to the internal reactions due to cases 1, 2, and 3, respectively. This leads to three homogeneous linear equations in w_1, w_2, and w_3. Only when cases 1, 2, and 3 have the same boundary conditions and are not coupled or are coupled by a fourth restraint that can be split off, as mentioned in the first case in item (5), does this lead to simple formulas for P_{cr} as expressed in terms of P_1, P_2, and P_3, such as those for composite columns coupled by elastic couplings with equal spacings (ref. 6). In other problems this method leads to a cubic equation for the buckling load P_{cr}. However, by combining the first two cases and then combining them with the third case (in ref. 13 such a case is presented, namely, the buckling of columns with T-sections), rather simple end formulas could be obtained containing square roots only.

(7) Accuracy of method: The method leads to exact results when the deflections w_n have the same shape, but sufficiently accurate results can be obtained if they differ in shape, as will be shown in this report.

As shown in reference 14, if $w_1, w_2, \ldots w_n$ differ in shape, the method remains exact if $P_1, P_2, \ldots P_n$ are considered as the

buckling loads belonging to the shapes of w_1 and w_2 in the component cases, as they occur in the combined case. Since, in general, these are not the optimum shapes that lead to the minimum buckling loads P_1 and P_2 as they occur in separate cases 1 and 2, by considering P_1 and P_2 as the minimum buckling loads conservative results will be obtained. However, if the structure is externally redundant, such as in the case of sandwich plates, there is another influence that may tend to make the method unconservative. This is the fact that in the composite case the boundary and continuity conditions have to be satisfied by the total deflection w only and not by the component deflections $w_1, w_2, \ldots w_n$ separately. This causes a relaxation of restraints that tends to make P_1 and P_2 smaller for the composite case than for the separate cases and thus to make the result unconservative. Hence in such a case the method may slightly overestimate the buckling load P_{cr} for the combined case.

(8) Problems where buckling deflection in one individual case is arbitrary: Let the case in which the buckling deflection is arbitrary be case 2. Then in the composite case the deflection w_2 for that case will have the same shape as w_1 for case 1. This may be understood as follows: If during the deformation for case 2 the shape of w_1 and hence the internal reaction for case 1 does not change, the internal reaction for the combined case will also be determined by the shape of w_1 (from items (4) and (6)). Hence, in order to make the external action equal the internal one at each point, the total deflection $w_1 + w_2$, and therefore w_2, must also have the same shape as w_1. In some cases, such as that of a sandwich column with asymmetric boundary conditions which will be considered in this report, the shape of w_1 for the combined case will differ from that for the individual case 1. However, also then, in order to obtain equal external and internal moments, in the combined case w_2 will have the same shape as w_1, but the shapes of w_1 and w_2 will differ from that of w_1 in the separate case 1. Exact results can be obtained by calculating P_1 and P_2 for the buckling deflections as they occur in the composite case.

(9) Columns or plates with initial deflections: The method may also be applied to columns or plates with initial deflections. Here one of the cases is the initial deflection with an individual buckling load equal to zero (refs. 1 and 15).

(10) Reduction to case of columns or plates on elastic foundation: In several problems it is convenient to reduce the restraint offered in

the component cases to that given by an equivalent elastic foundation. The structure then can be considered to be without any flexural or shearing rigidity but to be laterally supported by springs arranged in series with as many component springs as the number of cases into which its behavior is split. For example, if there are two cases, the springs consist of individual springs S_1 and S_2 (fig. 1).

PROBLEMS WHERE ALL COMPONENT CASES HAVE SAME BOUNDARY CONDITIONS

General Formulas

If all component cases have the same boundary conditions the resulting formula expressing the critical load in terms of the critical loads of the separate cases usually acquires the general form

$$P_{cr} = P_0 + P_r = P_0 + \left(P_1^{-1} + P_2^{-1} + P_3^{-1} + \ldots\right)^{-1} \tag{1}$$

where P_1, P_2, . . . P_n, are the critical loads of the separate cases and P_0 is the critical load that is due to the rigidity from the coupling case. For example, for a sandwich plate P_0 is the critical load from the proper flexural rigidity of the faces alone. Of course, this does not apply if only one mode is considered, such as in the case of homogeneous plates under nonhomogeneous stress distribution and that of the ultimate load of compressed plates, which is dealt with subsequently.

For plates where the rigidities in the X- and Y-directions differ a great deal, such as corrugated-core sandwich plates, it is possible and often necessary to allow for ratios w_2/w_1 of the component deflections which differ for the imaginary strips running in the X- and Y-directions of which the sandwich plate can be thought to be composed. This leads to a formula of the form

$$P_{cr} = P_0 + P_r = P_0 + \left(P_{1x}^{-1} + P_{2x}^{-1} + \ldots\right)^{-1} + \left(P_{1y}^{-1} + P_{2y}^{-1} + \ldots\right)^{-1} \tag{2}$$

Here the subscripts x and y refer to the buckling loads of the plate due to the rigidity of the X- and Y-strips, respectively, also taking account of the influence of the torsional moments acting on those strips.

This formula leads to accurate results for orthotropic sandwich plates and also to more accurate results than equation (1) for isotropic sandwich plates with different boundary conditions in the X- and Y-directions, such as long plates that are clamped at the unloaded edges.

Discussion and Derivation of Equation (1)

Equation (1), where in some cases P_0 is zero, was derived in references 3, 4, 6, and 11 for columns as well as for plates by applying items (1) to (6) and (8). In the case of columns the actions and reactions considered were the external and internal moments, and in the case of plates the transverse deflecting and restraining forces acting upon an element were compared. As stated in reference 11, this formula leads to accurate results if w_1, w_2, . . . w_n and w have the same shape.

However, even if w_1, w_2, . . . w_n and w are of different shapes sufficiently accurate results are obtained. In reference 14 the same formula was derived for the case in which w_1 and w_2 are different in shape by comparing the work done by deflecting and restraining forces. It was found that equation (1) is exact if in the combined case w_1 and w_2 have the same shape as they have in the component cases 1 and 2. But this is obviously so only if, in both the component and the combined cases, w_1, w_2, and w all have the same shape, since then, from items (3), (4), and (6), in the combined case the distribution of the deflecting and restraining forces will be similar. That is, if in the combined case the restraining forces from case 1 are given by $P_1 w_{1m} \Phi(x,y)$, where $\Phi(x,y)$ is a definite function of x and y, for case 2 they will be $P_2 w_{2m} \Phi(x,y)$ while the total deflecting forces will be $P_{cr} w_m \Phi(x,y)$. Here x and y are the coordinates in the plane of the plate, w_{1m} and w_{2m} are the maximum deflections from cases 1 and 2, and $w_m = w_{1m} + w_{2m}$ is the total deflection.

Perhaps a better insight into the physical meaning of the method of split rigidities may be obtained by deriving equation (1) by using item (10). Consider a long rectangular sandwich plate compressed in the X-direction with arbitrary boundary conditions at the loaded and unloaded edges (fig. 2). According to item (1) the buckling deflection w is split into case 1, from bending, with deflections w_1 and case 2, from shear deformation, with deflections w_2. However, as shown in the longitudinal section in figure 3, the shear deflection cannot occur

without bending of the faces (the bending rigidity of the core is neglected). This means that in the combined structure case 2 cannot occur without inducing a partial deformation according to case 1; in other words, cases 1 and 2 are coupled. According to item (5) one way to deal with this situation is to split off the coupling action. This means that in cases 1 and 2 the faces are assumed to have no proper flexural rigidity. Since, however, the buckling deflection of the two single faces requires a load equal to their proper buckling load P_0, from item (6) their deflection in the combined case will generate an extra load P_0 on the plate. Hence, this load P_0 has to be added to that from the combined cases 1 and 2. The combination of cases 1 and 2 is denoted as the reduced case. This procedure is exact if the buckling deflection of the single faces (case 0) is similar to the total buckling deflection w in the combined case.

In case 1 (deformation by bending only) the deflecting force acting on a small element $H\,dx\,dy$, where H is the total plate thickness (fig. 3), is

$$D_1 = -P_1 \frac{\partial^2 w_1}{\partial x^2}\,dx\,dy \tag{3}$$

where P_1 is the buckling load per unit width for case 1, neglecting the proper flexural rigidity of the faces. Hence from item (6) the restraining force is

$$R_1 = -P_1 \frac{\partial^2 w_1}{\partial x^2}\,dx\,dy \tag{4}$$

If the plate was supported by an elastic foundation with a foundation modulus C_1 the transverse restraining force acting upon an element $H\,dx\,dy$ would be $C_1 w_1\,dx\,dy$. Hence the restraint offered by the plate in case 1 is equivalent to that of an elastic foundation with a foundation modulus (spring constant)

$$C_1 = -P_1 \left.\frac{\partial^2 w_1}{\partial x^2}\right/ w_1 \tag{5}$$

In general, this spring constant may be a function of x and y.

Similarly, the equivalent spring constant for the restraint offered by the plate in case 2 (shear deformation of the core only) is

$$C_2 = -P_2 \frac{\partial^2 w_1}{\partial x^2} \Big/ w_2 \tag{6}$$

where P_2 is the buckling load per unit width for case 2. Hence, if with the actual buckling deflection w the partial deflections w_1 and w_2 have the same shape as in the individual cases 1 and 2, the reduced plate (without proper flexural rigidity of the faces) offers a restraint against buckling that is equivalent to the lateral restraint from two spring systems built in series with spring constants C_1 and C_2 (fig. 4(a)). Therefore, a unit lateral load per unit surface causes a deflection

$$w = \frac{1}{C_1} + \frac{1}{C_2} = \frac{1}{C_r} \tag{7}$$

so that the equivalent spring constant for the reduced plate is

$$C_r = \frac{C_1 C_2}{C_1 + C_2} = \left(C_1^{-1} + C_2^{-1} \right)^{-1} \tag{8}$$

The equivalent spring constant for case 0 (the single faces), with total buckling load P_0, is in the same way

$$C_0 = -P_0 \frac{\partial^2 w_0}{\partial x^2} \Big/ w_0 \tag{9}$$

Hence, if the actual buckling deflection w has the same shape as w_0 (for case 0 alone), the equivalent spring constant for the actual plate is

$$C = C_0 + C_r = C_0 + \frac{C_1 C_2}{C_1 + C_2} = C_0 + \left(C_1^{-1} + C_2^{-1} \right)^{-1} \tag{10}$$

that is, the spring in figure 4(b), with spring constant C, is equivalent to the spring system in figure 4(a).

A plate with a spring constant C will buckle if for any element the deflecting force $-P\frac{\partial^2 w}{\partial x^2}$ is equal to the restraining force Cw, so that the buckling load is

$$P_{cr} = -Cw\Big/\frac{\partial^2 w}{\partial x^2} \tag{11}$$

or, from equations (5), (6), (9), (10), and (11),

$$P_{cr} = \frac{w}{\partial^2 w/\partial x^2}\left\{P_0\frac{\partial^2 w_0/\partial x^2}{w_0} + \frac{P_1P_2\left(\partial^2 w_1/\partial x^2\right)\left(\partial^2 w_2/\partial x^2\right)/(w_1w_2)}{\left[P_1\left(\partial^2 w_1/\partial x^2\right)/w_1\right] + \left[P_2\left(\partial^2 w_2/\partial x^2\right)/w_2\right]}\right\}$$

$$= P_0\frac{\partial^2 w_0/\partial x^2}{\partial^2 w/\partial x^2}\frac{w}{w_0} + \frac{P_1P_2}{P_1\dfrac{\partial^2 w/\partial x^2}{\partial^2 w_2/\partial x^2}\dfrac{w_2}{w} + P_2\dfrac{\partial^2 w/\partial x^2}{\partial^2 w_1/\partial x^2}\dfrac{w_1}{w}} \tag{12}$$

With the aforementioned assumption that $w = w_0$, the first term to the right becomes P_0. The spring forces in the springs with constants C_1 and C_2 built in series are

$$C_1w_1 = C_2w_2 \tag{13}$$

so that from equations (5) and (6)

$$\frac{\partial^2 w_1/\partial x^2}{\partial^2 w_2/\partial x^2} = \frac{P_2}{P_1} \tag{14}$$

Further,

$$w = w_1 + w_2 \tag{15}$$

Using equations (14) and (15), in equation (12) the denominator of the second term to the right becomes

$$P_1 \frac{\partial^2 w/\partial x^2}{\partial^2 w_2/\partial x^2} \frac{w_2}{w} + P_2 \frac{\partial^2 w/\partial x^2}{\partial^2 w_1/\partial x^2} \frac{w_1}{w} = P_1\left(\frac{P_2}{P_1} + 1\right)\frac{w_2}{w} + P_2\left(1 + \frac{P_1}{P_2}\right)\frac{w_1}{w}$$

$$= \left(P_2 + P_1\right)\frac{w_2 + w_1}{w}$$

$$= P_1 + P_2 \tag{16}$$

Hence equation (12) transforms to

$$P_{cr} = P_0 + \frac{P_1 P_2}{P_1 + P_2} \tag{17}$$

which is identical to equation (1) with P_3 and so forth equal to zero. The more general equation (1) can be derived in the same way. Hence equation (1) is exact if w_1 and w_2 differ in shape, but if in the composite case $w_0 = w$, w_1 and w_2 have the same shape as in the separate cases 0, 1, and 2, respectively. This confirms the derivation in reference 14. However, as stated previously, this condition can be met only if w_0, w_1, and w_2 have the same shape. In the latter case equation (1) is exact within the limitations of the usual assumptions, such as neglect of the deformations from transverse shear in the faces and from normal stresses σ_z in planes parallel to the middle plane of the sandwich plate.

Sandwich Columns With Various Boundary Conditions

Calculations of buckling loads of sandwich plates with several boundary conditions were given in references 11, 12, and 14. In sandwich columns or wide plates compressed in the short direction, the author considered until now only the simply supported case (fig. 5(a)). Here the deflection w_1 for case 1, deformation from bending only, is a half sine wave. The buckling deflection w_2 from shear deformation alone (case 2) is arbitrary. Hence, from item (8), in the combined case w_1 and w_2 will both have the shape of a half sine wave. The single faces

(case 0) will also buckle in a half sine wave, so that, from item (6), in the combined case the internal moment is increased by a sinusoidal moment $P_0 w$, where P_0 is the buckling load of the faces. By adding a load P_0 to the buckling load P_r of the reduced case an external moment $P_0 w$ of the same amount is added, so that with a sinusoidal deflection w equilibrium is maintained in all cross sections. Hence equation (1) is exact for this case.

In reference 23, the author's method was extrapolated for calculating the buckling load of sandwich columns that are clamped at both ends or at one end (figs. 5(b) and 5(c)). It was found that for a strut that is clamped at both ends equation (1) yields exact results, but that for the simply supported clamped case (fig. 5(c)) equation (1) gives results that for two examples were unconservative by 5 and $6\frac{1}{2}$ percent.

This is understandable from the foregoing discussion. In the clamped-clamped case (fig. 5(b)) the buckling deflections w_0 and w_1 for the individual cases 0 and 1 are both full sine waves and the shape of w_2 is arbitrary. Hence, from item (8) and the above discussion, in the composite case w, w_1 and w_2 will also form full sine waves so that from item (1) the present method leads to exact results. Another way to see that equation (1) is exact for a clamped-clamped strut is to observe that the inflection points B and C are $(1/4)l$ and $(3/4)l$ from the left end. The line of action of the compressive force P_{cr} passes through these inflection points. The center part BC is in exactly the same condition as a simply supported strut with length $L = (1/2)l$ and the left and right parts AB and CD can be considered as the right and left parts of such a column, respectively (fig. 5(b)). Since P_{cr}, P_0, P_1, and P_2 in equation (1) also apply to this simply supported column with length L, this equation is also exact for the clamped-clamped column.

Consider now the clamped simply supported column of figure 5(c). For case 1 the buckling deflection is part of a sine wave, with the line of action of the compressive force as the axis. If the external and internal moments M_e and M_i are expressed in terms of the distance of the column to that axis, the equation $M_e = M_i$ becomes (fig. 6(a))

$$P_1 w_1 = -E_s I_s d^2 w_1 / dx^2 \tag{18}$$

This equation and the boundary conditions are satisfied by

$$w_1 = w_{1m} \sin \frac{\pi}{L} x \tag{19}$$

where L is the effective length AB_1 of the column (fig. 6(a)). The same applies to w_0 for case 0. Since for case 2 the deflection w_2 is arbitrary, from item (8) in the composite case it would have the same shape as w_1 and w. However, it may be easily seen that in the composite case w_1 has not the same shape as in the separate case 1. It is well known that in asymmetrically restrained, transversely loaded spans the distribution of the bending moments is changed by shear deflections as, for example, occurs in thin tubes or shells supported at three or more points. The effect of clamping a support diminishes. From figure 6(b), presenting the composite case, it is seen that the line of action AC_2 of the compressive force embraces an angle α with the original axis AC of the sandwich column. Hence at the clamped end C the transverse shear and the shear deformation is not zero, so that, although in case 1 (fig. 6(a)) the slope at C is zero, in the composite case the slope angle θ at C is not zero. Now, considering first the reduced case $(P_0 = 0)$, from the same reasoning as given in item (8), w_1, w_2, and w will have similar shapes with respect to the line of action of the compressive force but different shapes with respect to w_1 in case 1. Hence, from items (1) and (7) and the foregoing discussion, equation (1) is not exact if P_1 and P_2 are considered as the buckling loads for the separate cases 1 and 2. On the other hand it will be exact if P_1 and P_2 are the buckling loads for cases 1 and 2 as they occur in the reduced case of figure 6(b).

In the same way as shown for case 1 in figure 6(a), in figure 6(b) the deflections w_1 for case 1 are given by equation (19), so that w_2 and w will also vary simusoidally with respect to the line of action ABC_2 of the compressive force P_{cr}. Since at C the elastic line of the strut as shown by the solid curve embraces an angle with its original axis AC, the effective length L for the reduced case (fig. 6(b)) is greater, with respect to l, than in the separate case 1 (fig. 6(a)), where, as is well known, $L = 0.7l$. Therefore, in the actual case P_1 is smaller than it is for case 1 in figure 6(a). Since P_2 is independent of shape or length, it is the same as in the individual case 2. In reference 23, P_1 from the separate case 1 (fig. 6(a)) was used in equation (1), which explains why P_{cr} was found to be higher than the exact value (P_0 was assumed to be zero).

The effective length in figure 6(b) may be found in a similar way, as was shown on pages 70 to 78 of reference 6 for various problems, using the Haarman method. The deflections w_1, w_2, and w are measured

from the line of compression ABC_2. With the deflection w_1 at the clamped edge no rotation can occur with respect to the original axis AC, so that the tangent $C_1'C_1$ is parallel to AC. Hence from figure 6(b)

$$\alpha = -\left(\frac{dw_1}{dx}\right)_{x=l} = -\frac{1}{l}(w)_{x=l} \tag{20}$$

where w_1 is given by equation (19) and, since w has the same shape as was measured from ABC_2,

$$w = w_m \sin \frac{\pi}{L} x \tag{21}$$

Insertion of equations (19) and (21) into equation (20) gives

$$\tan \frac{\pi}{L} l = \frac{w_{1m}}{w_m} \frac{\pi}{L} l \tag{22}$$

From items (3), (4), and (6) the equality of external and internal moments requires that

$$P_r w = P_1 w_1 = P_2 w_2 \tag{23}$$

so that

$$\frac{w_{1m}}{w_m} = \frac{w_1}{w} = \frac{w_1}{w_1 + w_2} = \frac{P_2}{P_1 + P_2} \tag{24}$$

Since P_1 is equal to the P_1 for a simply supported strut of length L, from reference 11

$$P_1 = \frac{\pi^2 E_s I_s}{L^2} \tag{25}$$

where (fig. 3)

$$I_s = (1/2)h(t + h)^2 \tag{26}$$

and

$$P_2 = \frac{(t + h)^2}{t} G_c \tag{27}$$

where G_c is the modulus of rigidity of the core. Hence, from equations (22), (24), and (25), L has to be calculated from the following equation:

$$\tan \pi \frac{l}{L} = \frac{\pi P_2 l/L}{\frac{\pi^2 E_s I_s}{l^2}\left(\frac{l}{L}\right)^2 + P_2} \tag{28}$$

Then P_1 and P_2 follow from equations (25) and (27) and $P_{cr} = P_r$ from equation (1), with $P_0 = 0$ and $P_3, \ldots P_n = 0$. With the dimensions used in an example in reference 23, $E_s I_s = 43{,}200$ kg-cm^2, $P_2 = 360$ kilograms, and $l^2 = 800$ cm^2, equation (28) yields $l/L = 1.276$, so that $L^2 = l^2/1.628 = 491$ cm^2. Hence equation (25) gives $P_1 = 870$ kilograms, so that from equation (1), with $P_0 = 0$, $P_{cr} = 254$ kilograms. This is in accordance with the result obtained in reference 23 from an exact calculation, which shows that also for columns with asymmetric edge conditions equation (1) is exact if applied to the correct effective length of the column. However, for such cases, it loses the advantage of its simplicity.

Figure 6(b) illustrates what was said in reference 14 and under item (7). The deflections w_1 and w_2 satisfy the boundary conditions together and, as seen clearly from this figure, w_1 does not satisfy the boundary conditions. This relaxation of restraints causes P_1 to be smaller than P_1 from the separate case 1 alone (fig. 6(a)).

Usually P_0 is negligible, but if the bending rigidity of the faces is taken into account, one simply can calculate P_0 in equation (1) for the effective length L from equation (28), so that from reference 11

$$P_0 = \frac{\pi^2 E_s h^3}{6(1 - \nu^2)L^2} \tag{29}$$

Actually this makes equation (1) slightly conservative, since from figure 6(b) the deflection w has a sharp break at the clamped edge, so that P_0 actually will be slightly higher than would follow from equation (29).

Columns With Batten Plates and Latticed Columns

An application of equation (1) that shows some other features is the calculation of the critical stress of metal columns connected by batten plates with equal spacings (fig. 7(a)) or of timber columns that are coupled at equal distances (refs. 3 and 6). In many applications the deformation of the batten plates can be neglected. Then the buckling deflection can be split into two cases. Case 1 is caused by bending with respect to the common axis (fig. 7(b)). Case 2 is the deformation by shear, which bends the single columns between the batten plates in S-curves (fig. 7(c)). These deformations can occur independently of each other, so that

$$P_{cr} = \left(P_1^{-1} + P_2^{-1}\right)^{-1} \tag{30}$$

Including the plastic range, P_1 is sufficiently accurately given by

$$P_1 = \frac{\pi^2 E_t I}{l^2} \tag{31}$$

where

$$I = 2I_c + \left(Ah^2/4\right) \tag{32}$$

Here E_t is the tangent modulus, h is the spacing of the axes of inertia of the single columns, A is the total cross section of the composite column, and I_c is the moment of inertia of the single columns. In case 2 the batten plates translate with respect to each other without rotation (fig. 7(c)), so that

$$P_2 = \frac{2\pi^2 E_t I_c}{c_o^2} \tag{33}$$

where c_o is the effective free length of the single columns between two batten plates.

If also the deformation by shear and bending of the batten plates or wooden connections has to be taken into account, case 3 is added (fig. 7(d)). However, now cases 1 and 3 cannot occur independently, since the deflection w_3 for case 3 bends the single columns in a single half wave with respect to their original axes, which is part of the deformation in case 1. Therefore, according to item (5), the proper rigidity of the single columns is first assumed to be zero and subsequently its influence is added in the form of P_0. Hence, in equation (31) for P_1 the moment of inertia I is that of the reduced column,

$$I_r = Ah^2/4 \tag{34}$$

since I_c is assumed to be zero; P_2 remains as given by equation (33). From reference 6, assuming only the batten plates (or wooden connections) to deform, the individual buckling load for case 3 is

$$P_3 = \beta h^2/cv \tag{35}$$

where c is the center-to-center spacing of the batten plates and v is the translation of the single struts with respect to each other per unit shear force Q (fig. 7(d)). In reference 6 the factor β was calculated for several cases. If the rigidity of the end batten plates is half that of the intermediate ones, $\beta = 1$.

In the present problem P_0 is not equal to the buckling load of the single struts (in contrast to the case of a sandwich column, where it was equal to the buckling load of the faces), because during the deflection w_2 from case 2 (fig. 7(c)) no deflection in a single half wave occurs. The bending in S-curves between batten plates causes many inflection points to occur in the single struts, so that the internal moment in them is not increased. If the half-wave bending of the single struts occurred simultaneously with its total deflection w, from item (5) it would add a resistance in the longitudinal direction of the strut of $2\pi^2 E_t I_c/l^2$. However, since this half-wave bending occurs during the deflection $w - w_2$ only, its curvature reduces in the ratio $(w_2 - w)/w$, so that the added axial resistance is

$$P_0 = \frac{w - w_2}{w} \frac{2\pi^2 E_t I_c}{l^2} \tag{36}$$

Similarly to equation (23)

$$P_2 w_2 = P_r w \tag{37}$$

so that

$$\frac{w - w_2}{w} = 1 - \frac{P_r}{P_2} \tag{38}$$

and

$$P_0 = \left(1 - \frac{P_r}{P_2}\right) \frac{2\pi^2 E_t I_c}{l^2} \tag{39}$$

Since with a sufficiently large number of batten plates w_1 is distributed sinusoidally and since for w_2 and w_3 the buckling deflection at the batten plates is arbitrary, by the same reasoning as given in item (8) for one arbitrary component deflection in the composite case w, w_2, and w_3 will also have a generally sinusoidal half-wave distribution (actually, from ref. 24, if $c_o = c$, the centers of the batten plates are situated on a half sine wave).

From item (10) the column can be imagined as being without flexural rigidity and being laterally supported by a spring system as shown in figure 8. The equivalent spring constants are given by equations (5), (6), and (9) and by a similar equation for C_3. In the same way as shown for a spring system with spring constants C_0, C_1, and C_2, this leads to an equation like equation (1) which now contains a term with P_3. The requirements of items (1) and (7) for equation (1) to be exact are not entirely fulfilled here, since between the batten plates the elastic lines in the various cases are not exactly similar, although their overall shapes are those of half sine waves. They will be closer to that shape, the larger the number of batten plates. Equation (1) for this problem is

$$P_{cr} = P_0 + P_{cr} = P_0 + \left(P_1^{-1} + P_2^{-1} + P_3^{-1}\right)^{-1} \tag{40}$$

where P_0, P_1, P_2, and P_3 are given by equations (39), (31) with I replaced by I_r from equation (34), (33), and (35). Dividing by the cross section A gives

$$\sigma_{cr} = \sigma_0 + \sigma_r = \sigma_0 + \frac{\pi^2 E_t}{(l_r/r)^2} = \sigma_0 + \left(\sigma_1^{-1} + \sigma_2^{-1} + \sigma_3^{-1}\right)^{-1} \tag{41}$$

where l_r/r is the effective slenderness of the reduced case,

$$\left.\begin{aligned} \sigma_1 &= \frac{\pi^2 E_t}{(l/r)^2} \\ \sigma_2 &= \frac{\pi^2 E_t}{(c_o/r_c)^2} \\ \sigma_3 &= \frac{\beta h^2}{cvA} \end{aligned}\right\} \tag{42}$$

and

$$r^2 = I_r/A = h^2/4 \tag{43}$$

From equations (39), (41), and (42),

$$\sigma_0 = \left(1 - \frac{\sigma_r}{\sigma_2}\right)\frac{\pi^2 E_t}{(l/r_c)^2} = \left[1 - \left(\frac{c_o/r_c}{l_r/r}\right)^2\right]\frac{\pi^2 E_t}{(l/r_c)^2} \tag{44}$$

As shown more extensively in reference 6, equation (41) may be written as

$$\sigma_{cr} = \frac{\pi^2 E_t}{(l_{eq}/r)^2} \tag{45}$$

where the effective slenderness l_{eq}/r is given by

$$\left(\frac{l_{eq}}{r}\right)^2 = \frac{\left(l_r/r\right)^2}{1 + \left[\left(l_r/r\right)^2 - \left(c_o/r_c\right)^2\right]\left(r_c/l\right)^2} \tag{46}$$

From equations (41) and (42)

$$\left(l_r/r\right)^2 = \left(l/r\right)^2 + \left(c_o/r_c\right)^2 + \left[\pi^2 E_t A c v/\left(\beta h^2\right)\right] \tag{47}$$

With connections of vanishing rigidity, the factor v in equation (47) becomes infinite, so that equation (46) yields the correct result, namely, that the effective slenderness is equal to that of the single struts l/r_c. In contrast, for example, equations (348) to (350) of reference 25 and equations (96) and (97) of reference 26 for infinitely weak connections yield zero buckling loads. From figures 7(c) and 7(d) a batten plate at the center of a column has no effect, so that for a column with end connections only, one has to assume that the spacing of the batten plates is $c = l/2$.

An exact formula for the buckling stress of these columns has been derived in reference 24 for the case in which $c_o = c$ and the rigidity of the end plates is half that of the intermediate ones. Changing the reduced modulus to the tangent modulus E_t gives the buckling condition

$$\frac{h^2}{2r_c^2} = \frac{2\pi}{m} \frac{\cos\frac{\pi}{n} - \cos\frac{\pi}{m}}{\left(1 - \cos\frac{\pi}{n}\right)\sin\frac{\pi}{m}} \left[1 + \frac{E_t A v}{2c}\left(1 - \cos\frac{\pi}{n}\right)\right] \tag{48}$$

where $n = l/c$ and $m = \left(l_{eq}/r\right)/\left(c/r_c\right)$. For this same case, in equations (46) and (47) $c_o = c$ and $\beta = 1$. Table V of reference 6, given as table 1 herein, contains some values of m calculated from equations (46) and (47) as well as from equation (48) by Mr. Lie Han Yang. It refers to timber columns built up from single struts with dimensions 8 by 20 centimeters, the smaller dimension being that parallel to the plane of bending; E_t was assumed to be 100,000 kg/cm^2. Table 1 shows that equation (46) is conservative and indeed is more accurate for large numbers n than for small ones. The general accuracy is very satisfactory.

Similar formulas were derived in reference 6 for latticed columns, coupled by diagonals only (fig. 9(a)) or by diagonals and verticals (fig. 9(b)), using equation (1) with $P_3, \ldots P_n$ equal to zero. If I is replaced by I_r from equation (34), P_1 is given by equation (31); P_0 represents the axial resistance of the single columns, so that

$$P_0 = \frac{2\pi^2 E_t I_c}{l^2} \tag{49}$$

In order to find P_2 it is observed that for case 2, where the single columns are assumed to be infinitely rigid against axial strain, a slope β of the column with respect to its original axis causes a transverse shear force $Q = P_2\beta$ that has to be resisted by the lacing. Denoting as Q' the fictitious transverse shear force that would cause a unit angular distortion, the equation $Q = Q'\beta$ is obtained, so that

$$P_2 = Q' \tag{50}$$

Inserting P_0, P_1, and P_2 into equation (1) gives

$$P_{cr} = \frac{\pi^2 E_t}{l^2}\left[2I_c + \frac{l^2}{l^2 + \left(\pi^2 E_t I_r/Q'\right)} I_r\right] \tag{51}$$

As may be easily checked, for a column with diagonals only (fig. 9(a))

$$Q' = EA_d \sin^2\alpha \cos\alpha \tag{52}$$

where A_d is the cross section of the diagonals. For the arrangement shown in figure 9(b)

$$1/Q' = \left[1\Big/\left(EA_d \sin^2\alpha \cos\alpha\right)\right] + \left(\tan\alpha/EA_v\right) \tag{53}$$

where A_v is the cross section of the verticals. For both these cases an upper limit for P_{cr} is that of the single struts with a free length c and slenderness c/r_s. With diagonal cross sections $A_d = 0$, equations (52) and (53) yield $Q' = 0$ and equation (51) reduces correctly

to the critical load of the single columns, in contrast with equations (335) to (339) of reference 25 and equations (93) and (94) of reference 26 which yield $P_{cr} = 0$.

Sandwich Plates With Orthotropic Core

A comprehensive discussion on the application of equation (1) to the elastic and plastic buckling of sandwich plates was given in references 11, 12, and 14. It was shown that equation (1) is exact if w_1, w_2, and w have the same shape, such as occurs for a compressed long plate with simply supported unloaded edges. In that case the requirements for exactness, stated in item (1), are satisfied. For a long plate with simply supported long edges that is subjected to shear, the deflections w_1 and w_2 differ somewhat, but nevertheless results obtained in references 22, 23, and 27 differ less than 1 percent from those from equation (1). This is due to the fact that, although w_1 and w_2 differ in shape, the rigidities of imaginary X- and Y-strips (parallel and perpendicular to the long edges) are still of the same order of magnitude being simply supported at the nodal lines and at the long edges, respectively.

A more intricate case arises if for one of the component cases the strips running in the X-direction (the X-strips) have a rigidity that differs from that of the Y-strips (fig. 10(a)). For isotropic sandwich plates this occurs for a long compressed plate that has clamped unloaded edges. For case 1 (deformation from bending) the clamped Y-strips are much more rigid than the X-strips, which can be assumed to be simply supported at the transverse nodal lines. On the other hand, in case 2 (deformation by transverse shear forces) in any buckle both X- and Y-strips deflect in half sine waves so that their rigidities are of the same order of magnitude. As explained in reference 14 and item (7), for cases where w_1 and w_2 differ in shape two influences occur, one that tends to make equation (1) conservative and another that tends to make it unconservative. In the present case the latter influence, due to the fact that the boundary and continuity conditions have to be satisfied by the total deflection $w = w_1 + w_2$ and not by w_1 and w_2 separately, is predominant, making equation (1) unconservative by 7 percent (ref. 28).

Apparently the fact that in the combined case w_1 and w_2 do not satisfy the boundary conditions separately is mainly due to the difference in rigidity of X- and Y-strips and not to the difference in shape of the deflections w_1 and w_2. By prescribing a constant ratio w_{2m}/w_{1m} for the amplitudes of the deflections in cases 2 and 1, one prescribes that the ratio w_{2xm}/w_{1xm} of the amplitudes of the center X-strip is

equal to the ratio w_{2ym}/w_{1xm} of the amplitudes of the center Y-strip. Actually in the composite case this cannot be true. If w_{2xm}/w_{1xm} is equal to α, w_{2ym}/w_{1ym} will be much more than α because of the clamping of the Y-strips since w_{1ym} is and w_{2ym} is not affected by the clamping, as explained previously. Hence, with a prescribed ratio $w_{2m}/w_{1m} = w_{2xm}/w_{1xm} = w_{2ym}/w_{1ym}$, one could imagine that for the center Y-strip w_{2y} has negative end deflections $-w_{2p}$ and w_{1y} has positive end deflections $w_{1p} = w_{2p}$ (fig. 10(b)). Then the boundary conditions at $y = 0$ and $y = b$ are satisfied by $w = w_1 + w_2 = w_{1p} - w_{2p} = 0$, while the ratio w_{2ya}/w_{1ya} of the amplitudes of the actual deflections is more than the ratio w_{2ym}/w_{1ym}, as it should be. This shows the relaxation of restraints for the component cases 1 and 2, which makes the actual buckling load smaller than that obtained from equation (1).

Although for isotropic plates with different rigidities of X- and Y-strips equation (1) is still sufficiently accurate, for sandwich plates with anisotropic core, where the ratio G_y/G_x differs too much from 1, as stated in reference 14, equation (1) becomes too inaccurate. From the preceding discussion, the obvious way to improve this situation is to admit a ratio w_{2ym}/w_{1ym} for the Y-strips that differs from the ratio w_{2xm}/w_{1xm} for the X-strips. This leads to equation (2) that will be shown to give accurate results for anisotropic sandwich plates and also more accurate results than equation (1) for isotropic sandwich plates. Equation (2) will now be derived.

Derivation of Equation (2)

Consider a long sandwich plate with isotropic faces, an orthotropic core compressed in the long (X) direction, and arbitrary boundary conditions at the unloaded edges (fig. 11). After splitting off the proper rigidity of the faces (item (5)) the plate is considered as a grid consisting of X- and Y-strips, but due account is taken of the restraints exerted upon these strips by the twisting moments along their long edges. This same method was applied by the author in reference 29 and in earlier papers for deriving simple formulas for the bending moments in rectangular plates under several loading and boundary conditions. From item (1) the deflections of these strips are split into those from bending about the common middle plane (case 1) and from transverse shear (case 2).

Let the lateral restraint offered by the X-strips in cases 1 and 2 (cases 1x and 2x) and that of the Y-strips in cases 1 and 2 (cases 1y and 2y) be equivalent to that of elastic foundations with foundation moduli of C_{1x}, C_{2x}, C_{1y}, and C_{2y}, respectively. Hence, if in the

composite case the deflections from cases 1 and 2 have the same shape as in the individual cases, from equation (8) the equivalent spring constant of the reduced plate is

$$C_r = C_x + C_y = \left(C_{1x}^{-1} + C_{2x}^{-1}\right)^{-1} + \left(C_{1y}^{-1} + C_{2y}^{-1}\right)^{-1} \tag{54}$$

because the resistances of X- and Y-strips just act additively. The equivalent spring constant of the actual plate which is similar to equation (10) is

$$C = C_0 + C_r = C_0 + \left(C_{1x}^{-1} + C_{2x}^{-1}\right)^{-1} + \left(C_{1y}^{-1} + C_{2y}^{-1}\right)^{-1} \tag{55}$$

where C_0 is the equivalent spring constant for the proper rigidity of the faces (case 0). The equivalent spring system is shown schematically in figure 12. Using equations similar to equations (5), (6), (9), (13), and (14), where the subscripts 1 or 2 are replaced by 1x and 1y or 2x and 2y, in a way similar to that in which equation (10) reduced to equation (1), equation (55) reduces to equation (2). In equation (2) P_0, P_{1x}, P_{2x}, P_{1y}, and P_{2y} are the buckling loads for the individual cases 0, 1x, 2x, 1y, and 2y, respectively. Similarly to equation (1), equation (2) is exact if the component deflections w_0, w_{1x}, w_{2x}, w_{1y}, and w_{2y} for these cases have the same shape and if these shapes are the same in the composite case as in the separate cases. Since for case 2, for simply supported as well as for clamped edges, the X- and Y-strips deflect in half sine waves (refs. 5 and 12), equation (2) will be exact for simply supported isotropic or orthotropic sandwich plates, where for case 1 the deflections have this same shape. However, as will be shown, for other boundary conditions also equation (2) is very accurate (maximum discrepancy about 3 percent).

Application of Equation (2) to Orthotropic Sandwich Plates With Simply Supported Edges

Equation (2) can be applied to orthotropic sandwich plates with simply supported edges as follows. The restraining force exerted by an X-strip per unit plate surface can be written as (fig. 13)

$$R_x = -\frac{\partial Q_x}{\partial x} \tag{56}$$

where Q_x is the transverse shear per unit width of the strip. From equation (102) of reference 30, for case 1 (bending only), by adding the subscript 1,

$$Q_{1x} = \frac{\partial M_{1x}}{\partial x} + \frac{\partial M_{1yx}}{\partial y} \tag{57}$$

and in the same way from equation (37) of reference 30

$$M_{1x} = -N_s\left(\frac{\partial^2 w_{1x}}{\partial x^2} + \nu \frac{\partial^2 w_{1y}}{\partial y^2}\right) \tag{58}$$

where N_s is the flexural rigidity of the reduced sandwich plate, and ν is Poisson's ratio. As explained previously for the reduced case the proper flexural rigidity of the faces is neglected. The bending rigidity of the core is always negligible, so that (fig. 3)

$$N_s = \frac{E_s h(t + h)^2}{2\left(1 - \nu^2\right)} \tag{59}$$

where E_s is the modulus of elasticity of the faces (skin). From the equations on page 11 of reference 31 it follows that, using again the subscript 1 for case 1,

$$M_{1yx} = -M_{1xy} = -D_{1xy}\left(\frac{\partial^2 w}{\partial x\, \partial y} - \frac{1}{2}\frac{\partial \gamma x}{\partial y} - \frac{1}{2}\frac{\partial \gamma y}{\partial x}\right)$$

The shear angles γx and γy can be expressed in terms of the deflections w_{2x} and w_{2y} for case 2 occurring from shear alone, since obviously

$$\left.\begin{aligned} \gamma x &= \frac{\partial w_{2x}}{\partial x} \\ \gamma y &= \frac{\partial w_{2y}}{\partial y} \end{aligned}\right\} \tag{60}$$

Further, since the faces are isotropic, the ratio D_{1xy} of the twisting moment to twist is $N_s(1 - \nu)$ as it is for an isotropic plate, so that

$$M_{1yx} = -N_s(1 - \nu)\left(\frac{\partial^2 w}{\partial x\,\partial y} - \frac{1}{2}\frac{\partial^2 w_{2x}}{\partial x\,\partial y} - \frac{1}{2}\frac{\partial^2 w_{2y}}{\partial x\,\partial y}\right) \tag{61}$$

Since

$$\left.\begin{aligned} w_{2x} &= w - w_{1x} \\ w_{2y} &= w - w_{1y} \end{aligned}\right\} \tag{62}$$

$$M_{1yx} = -\frac{1}{2} N_s(1 - \nu)\left(\frac{\partial^2 w_{1x}}{\partial x\,\partial y} + \frac{\partial^2 w_{1y}}{\partial x\,\partial y}\right) \tag{63}$$

Insertion of equations (58) and (63) into equation (57) and of the latter into equation (56) yields for case 1

$$R_{1x} = -\frac{\partial^2 M_{1x}}{\partial x^2} - \frac{\partial^2 M_{1yx}}{\partial x\,\partial y} = N_s\left[\frac{\partial^4 w_{1x}}{\partial x^4} + \frac{1}{2}(1 - \nu)\frac{\partial^4 w_{1x}}{\partial x^2 \partial y^2} + \frac{1}{2}(1 + \nu)\frac{\partial^4 w_{1y}}{\partial x^2 \partial y^2}\right] \tag{64}$$

If the lateral restraint given by the X-strips in case 1 was given by an imaginary elastic foundation with a foundation modulus C_{1x}, R_{1x} would be equal to $C_{1x}w_{1x}$ so that the equivalent spring constant is

$$C_{1x} = \frac{R_{1x}}{w_{1x}} = \frac{N_s}{w_{1x}}\left[\frac{\partial^4 w_{1x}}{\partial x^4} + \frac{1}{2}(1 - \nu)\frac{\partial^4 w_{1x}}{\partial x^2 \partial y^2} + \frac{1}{2}(1 + \nu)\frac{\partial^4 w_{1y}}{\partial x^2 \partial y^2}\right] \tag{65}$$

Similarly the equivalent spring constant for the Y-strips in case 1 is

$$C_{1y} = \frac{R_{1y}}{w_{1y}} = \frac{N_s}{w_{1y}}\left[\frac{\partial^4 w_{1y}}{\partial y^4} + \frac{1}{2}(1 - \nu)\frac{\partial^4 w_{1y}}{\partial x^2 \partial y^2} + \frac{1}{2}(1 + \nu)\frac{\partial^4 w_{1x}}{\partial x^2 \partial y^2}\right] \tag{66}$$

The moduli of rigidity of the core against transverse shear forces Q_x and Q_y are denoted as G_x and G_y, respectively. From equations (6) and (7) of part I of reference 5, Q_x and Q_y for case 2 can be expressed as

$$\left.\begin{aligned} Q_{2x} &= \frac{(t+h)^2}{t} G_x \frac{\partial w_{2x}}{\partial x} \\ Q_{2y} &= \frac{(t+h)^2}{t} G_y \frac{\partial w_{2y}}{\partial y} \end{aligned}\right\} \tag{67}$$

so that, using equation (56) and analogous to equations (65) and (66),

$$\left.\begin{aligned} C_{2x} &= \frac{R_{2x}}{w_{2x}} = -\frac{1}{w_{2x}} \frac{\partial Q_{2x}}{\partial x} = -\frac{(t+h)^2}{t} \frac{G_x}{w_{2x}} \frac{\partial^2 w_{2x}}{\partial x^2} \\ C_{2y} &= \frac{R_{2y}}{w_{2y}} = -\frac{1}{w_{2y}} \frac{\partial Q_{2y}}{\partial y} = -\frac{(t+h)^2}{t} \frac{G_y}{w_{2y}} \frac{\partial^2 w_{2y}}{\partial y^2} \end{aligned}\right\} \tag{68}$$

For a long plate with simply supported unloaded edges the boundary conditions are satisfied if

$$\frac{w}{w_m} = \frac{w_0}{w_{0m}} = \frac{w_{1x}}{w_{1xm}} = \frac{w_{2x}}{w_{2xm}} = \frac{w_{1y}}{w_{1ym}} = \frac{w_{2y}}{w_{2ym}} = \sin \frac{\pi}{a} x \sin \frac{\pi}{b} y \tag{69}$$

Inserting this into equations (65), (66), and (68) gives

$$\left.\begin{aligned} C_{1x} &= \frac{\pi^4}{b^4} N_s \left[\frac{1}{\beta^4} + \frac{1}{2}(1-\nu) \frac{1}{\beta^2} + \frac{1}{2}(1+\nu) \frac{\theta_y}{\theta_x \beta^2} \right] \\ C_{1y} &= \frac{\pi^4}{b^4} N_s \left[1 + \frac{1}{2}(1-\nu) \frac{1}{\beta^2} + \frac{1}{2}(1+\nu) \frac{\theta_x}{\theta_y \beta^2} \right] \end{aligned}\right\} \tag{70}$$

$$\left.\begin{aligned} C_{2x} &= \frac{\pi^2}{b^2}\frac{(t+h)^2}{t}G_x\frac{1}{\beta^2} \\ C_{2y} &= \frac{\pi^2}{b^2}\frac{(t+h)^2}{t}G_y \end{aligned}\right\} \tag{71}$$

where a is the half wave length in the X-direction,

$$\beta = a/b \tag{72}$$

and

$$\left.\begin{aligned} \theta_x &= \frac{w_{1xm}}{w_m} \\ \theta_y &= \frac{w_{1ym}}{w_m} \end{aligned}\right\} \tag{73}$$

From figure 12, since the springs with constants C_{1x} and C_{2x} have to carry the same load,

$$C_{1x}w_{1xm} = C_{2x}w_{2xm} \tag{74}$$

so that

$$\theta_x = \frac{w_{1xm}}{w_{1xm} + w_{2xm}} = \frac{C_{2x}}{C_{1x} + C_{2x}} \tag{75}$$

Similarly

$$\theta_y = \frac{w_{1ym}}{w_{1ym} + w_{2ym}} = \frac{C_{2y}}{C_{1y} + C_{2y}} \tag{76}$$

Inserting C_{1x} and C_{2x} from equations (70) and (71) into equation (75) gives

$$\theta_x = \frac{1}{1 + r_x\left(\frac{1}{\beta^2} + \frac{1-\nu}{2} + \frac{1+\nu}{2}\frac{\theta_y}{\theta_x}\right)} \tag{77}$$

where

$$r_x = \frac{\pi^2 N_s t}{b^2 G_x (t + h)^2} \tag{78}$$

Equation (77) can be written as

$$\left[1 + \left(\frac{1}{\beta^2} + \frac{1 - \nu}{2}\right) r_x\right] \theta_x + \frac{1 + \nu}{2} r_x \theta_y = 1 \tag{79}$$

From equations (70), (71), and (76)

$$\theta_y = \frac{1}{1 + r_y \left(1 + \frac{1 - \nu}{2} \frac{1}{\beta^2} + \frac{1 + \nu}{2} \frac{\theta_x}{\theta_y \beta^2}\right)} \tag{80}$$

where

$$r_y = \frac{\pi^2 N_s t}{b^2 G_y (t + h)^2} \tag{81}$$

Equation (80) is written as

$$\frac{1 + \nu}{2} r_y \theta_x + \left[\beta^2 + \left(\beta^2 + \frac{1 - \nu}{2}\right) r_y\right] \theta_y = \beta^2 \tag{82}$$

Solving equations (79) and (82) for θ_x and θ_y,

$$\left.\begin{aligned} \theta_x &= \frac{\left[\beta^2 + \left(\beta^2 + \frac{1 - \nu}{2}\right) r_y\right] - \frac{1 + \nu}{2} \beta^2 r_x}{\left[1 + \left(\frac{1}{\beta^2} + \frac{1 - \nu}{2}\right) r_x\right]\left[\beta^2 + \left(\beta^2 + \frac{1 - \nu}{2}\right) r_y\right] - \frac{1}{4} (1 + \nu)^2 r_x r_y} \\ \theta_y &= \frac{\left[1 + \left(\frac{1}{\beta^2} + \frac{1 - \nu}{2}\right) r_x\right] \beta^2 - \frac{1 + \nu}{2} r_y}{\left[1 + \left(\frac{1}{\beta^2} + \frac{1 - \nu}{2}\right) r_x\right]\left[\beta^2 + \left(\beta^2 + \frac{1 - \nu}{2}\right) r_y\right] - \frac{1}{4} (1 + \nu)^2 r_x r_y} \end{aligned}\right\} \tag{83}$$

In equation (2) P_0 is the buckling load of the faces if buckling alone occurs, so that, from equation (g) on page 329 of reference 26

$$P_0 = \frac{2\pi^2 N}{b^2}\left(\frac{1}{\beta} + \beta\right)^2 \tag{84}$$

where N is the flexural rigidity of each of the faces. Further, in equation (2), in connection with equations (5), (6), (69), and (75),

$$\left(P_{1x}^{-1} + P_{2x}^{-1}\right)^{-1} = \frac{P_{1x}P_{2x}}{P_{1x} + P_{2x}} = \frac{C_{2x}}{C_{1x} + C_{2x}} P_{1x} = \theta_x P_{1x} \tag{85}$$

Similarly

$$\left(P_{1y}^{-1} + P_{2y}^{-1}\right)^{-1} = \theta_y P_{1y} \tag{86}$$

From equations (5) and (69)

$$\left.\begin{aligned} P_{1x} &= \frac{a^2}{\pi^2} C_{1x} \\ P_{1y} &= \frac{a^2}{\pi^2} C_{1y} \end{aligned}\right\} \tag{87}$$

Hence equation (2) can be written as

$$P_{cr} = \frac{2\pi^2 N}{b^2}\left(\frac{1}{\beta} + \beta\right)^2 + \frac{a^2}{\pi^2}\left(\theta_x C_{1x} + \theta_y C_{1y}\right) \tag{88}$$

which result could also have been obtained from equation (55) in combination with equations (9), (11), (69), (75), (76), and (84). Using equation (70), equation (88) yields

$$P_{cr} = \frac{2\pi^2 N}{b^2}\left(\frac{1}{\beta} + \beta\right)^2 + \frac{\pi^2 N_s}{b^2}\left[\left(\frac{1}{\beta^2} + 1\right)\theta_x + \left(1 + \beta^2\right)\theta_y\right] \tag{89}$$

where θ_x and θ_y are given by equation (83). As stated previously, this result is exact. This will be shown in the next section by comparison of a more general formula with the results obtained in reference 32. For isotropic core $G_x = G_y = G$ and $r_x = r_y = r$, so that from equation (83)

$$\theta_x = \theta_y = \theta = \frac{\beta^2 + \frac{1 - \nu}{2}\left(1 + \beta^2\right)r}{\beta^2 + \frac{3 - \nu}{2}\left(1 + \beta^2\right)r + \frac{1 - \nu}{2}\left(\frac{1}{\beta} + \beta\right)^2 r^2} \tag{90}$$

and equation (89) becomes

$$P_{cr} = \frac{\pi^2}{b^2}\left(\frac{1}{\beta} + \beta\right)^2\left(2N + \theta N_s\right) \tag{91}$$

This result can be shown to be identical to that given by equation (31) of reference 11 for $\eta = 1$ (elastic range).

Plastic Buckling of Corrugated Core Sandwich Plates, Hinged or Clamped at Unloaded Edges

A cross section of the plate is given in figure 14. Considering first case 1 (bending only), from equation (30) of reference 33 or equation (22) of reference 34 the bending moment M_y from bending about the middle plane of the sandwich and carried by the faces, considered as membranes only, is

$$M_{1y} = -E_s I_s\left(B\frac{\partial^2 w_{1x}}{\partial x^2} + D\frac{\partial^2 w_{1y}}{\partial y^2}\right) \tag{92}$$

where (fig. 3)

$$I_s = \frac{1}{2}h(t + h)^2 \tag{93}$$

For obtaining M_{1x} the moment $-E_{tc}I_c\left(\partial^2 w_{1x}/\partial x^2\right)$ taken by the corrugation cross section, where E_{tc} is the tangent modulus of the corrugation material, must be added to the moment carried by the faces. Hence, using again the same equations from references 33 or 34,

$$M_{lx} = -E_s I_s \left(A \frac{\partial^2 w_{lx}}{\partial x^2} + B \frac{\partial^2 w_{ly}}{\partial y^2} \right) - E_{tc} I_c \frac{\partial^2 w_{lx}}{\partial x^2}$$

$$= -E_s I_s \left[\left(A + \mu \frac{E_{tc}}{E_c} \right) \frac{\partial^2 w_{lx}}{\partial x^2} + B \frac{\partial^2 w_{ly}}{\partial y^2} \right] \tag{94}$$

where

$$\mu = \frac{E_c I_c}{E_s I_s} \tag{95}$$

and E_c is the elastic modulus of the corrugation material. From the same references the ratio $N_s(1 - \nu)$ of the twisting moment to twist in the plastic range changes to $2E_s I_s F$ so that, instead of the present equation (63),

$$M_{lyx} = -E_s I_s F \left(\frac{\partial^2 w_{lx}}{\partial x \, \partial y} + \frac{\partial^2 w_{ly}}{\partial x \, \partial y} \right) \tag{96}$$

The plastic parameters A, B, D, and F are given by equations (22) to (24) of reference 33 and equations (21) or (21a) of reference 34. Using equations (94) and (96) gives, instead of equation (64),

$$R_{lx} = - \frac{\partial^2 M_{lx}}{\partial x^2} - \frac{\partial^2 M_{lyx}}{\partial x \, \partial y}$$

$$= E_s I_s \left[\left(A + \mu \frac{E_{tc}}{E_c} \right) \frac{\partial^4 w_{lx}}{\partial x^4} + B \frac{\partial^4 w_{ly}}{\partial x^2 \, \partial y^2} + F \left(\frac{\partial^4 w_{lx}}{\partial x^2 \, \partial y^2} + \frac{\partial^4 w_{ly}}{\partial x^2 \, \partial y^2} \right) \right] \tag{97}$$

from which, instead of equation (65),

$$C_{lx} = \frac{R_{lx}}{w_{lx}} = \frac{E_s I_s}{w_{lx}} \left[\left(A + \mu \frac{E_{tc}}{E_c} \right) \frac{\partial^4 w_{lx}}{\partial x^4} + F \frac{\partial^4 w_{lx}}{\partial x^2 \, \partial y^2} + (B + F) \frac{\partial^4 w_{ly}}{\partial x^2 \, \partial y^2} \right] \tag{98}$$

In the same way, using equations (92) and (96) gives

$$C_{1y} = \left(- \frac{\partial^2 M_{1y}}{\partial y^2} - \frac{\partial^2 M_{1yx}}{\partial x \, \partial y} \right) \Bigg/ w_{1y} = \frac{E_s I_s}{w_{1y}} \left[D \frac{\partial^4 w_{1y}}{\partial y^4} + F \frac{\partial^4 w_{1y}}{\partial x^2 \, \partial y^2} + (B + F) \frac{\partial^4 w_{1x}}{\partial x^2 \, \partial y^2} \right] \tag{99}$$

Let the deflections now be, as was done for laterally loaded slabs in reference 35 and for a stability problem in reference 36,

$$\left. \begin{aligned} w_{1x} &= Y_x \sin \frac{\pi}{a} x \\ w_{1y} &= Y_y \sin \frac{\pi}{a} x \end{aligned} \right\} \tag{100}$$

where

$$\left. \begin{aligned} Y_x &= \sum w_{xm} u_m \\ Y_y &= \sum w_{ym} u_m \end{aligned} \right\} \tag{101}$$

Here w_{xm} and w_{ym} are constants and the u_m are the normal functions that automatically satisfy the boundary conditions at the unloaded edges, since they represent the modes of vibration of a Y-strip. These functions have the general form (ref. 37)

$$u_m = C_1 \left(\cos \alpha_m y + \cosh \alpha_m y \right) + C_2 \left(\cos \alpha_m y - \cosh \alpha_m y \right) +$$

$$C_3 \left(\sin \alpha_m y + \sinh \alpha_m y \right) + C_4 \left(\sin \alpha_m y - \sinh \alpha_m y \right) \tag{102}$$

so that

$$\left.\begin{aligned} \frac{d^4 u_m}{dy^4} &= \alpha_m{}^4 u_m \\ \frac{d^2 u_m}{dy^2} &= \alpha_m{}^2 \bar{u}_m \end{aligned}\right\} \tag{103}$$

However, since the functions u_m are orthogonal, $\bar{u}_m \neq u_m$ can be developed in a series of u_m:

$$\bar{u}_m = k_{1m}u_1 + k_{2m}u_2 + k_{3m}u_3 + \cdots \tag{104}$$

It appears sufficiently accurate to use only the first terms of equations (101) and (104). Hence

$$\frac{d^2 u_1}{dy^2} = \alpha_1{}^2 \bar{u}_1 = \alpha_1{}^2 k_{11} u_1 \tag{105}$$

Insertion of equations (100), (101), (103), and (105) into equation (98) gives

$$C_{lx} = \frac{E_s I_s}{Y_x}\left[\left(A + \mu \frac{E_{tc}}{E_c}\right)\frac{\pi^4}{a^4} Y_x - F\frac{\pi^2}{a^2}\frac{d^2 Y_x}{dy^2} - (B + F)\frac{\pi^2}{a^2}\frac{d^2 Y_y}{dy^2}\right]$$

$$= \frac{\pi^4}{b^4} E_s I_s \left\{\left(A + \mu \frac{E_{tc}}{E_c}\right)\frac{1}{\beta^4} - \frac{b^2 \alpha_1{}^2 k_{11}}{\pi^2 \beta^2}\left[F + (B + F)\frac{\theta_y}{\theta_x}\right]\right\} \tag{106}$$

Similarly one obtains from equation (99)

$$C_{ly} = \frac{\pi^4}{b^4} E_s I_s \left\{\frac{\alpha_1{}^4 b^4}{\pi^4} D - \frac{b^2 \alpha_1{}^2 k_{11}}{\pi^2 \beta^2}\left[F + (B + F)\frac{\theta_x}{\theta_y}\right]\right\} \tag{107}$$

Instead of calculating α_1 and k_{11} for various boundary conditions, it may be observed that, if one or two of the unloaded edges are either simply supported or clamped, from equation (41) of reference 12, the buckling load of a homogeneous plate is

$$P_h = \frac{\pi^2}{b^2} EI\left[\frac{A}{\beta^2} + p(B + 2F) + qD\beta^2\right] \tag{108}$$

where p and q are given in table 1 of reference 11. Hence, with

$$w = Y \sin \frac{\pi}{a} x \tag{109}$$

where Y is a function of y alone, the equivalent spring constant is, analogous to equation (5),

$$C = -P_h \frac{\partial^2 w}{\partial x^2}\Big/ w = \frac{\pi^2}{a^2} P_h = \frac{\pi^4}{b^4} EI\left[\frac{A}{\beta^4} + p(B + 2F)\frac{1}{\beta^2} + qD\right] \tag{110}$$

From equations (106) and (107) for a homogeneous plate, where $\theta_y/\theta_x = 1$ and $\mu = 0$,

$$C = C_{1x} + C_{1y} = \frac{\pi^4}{b^4} E_s I_s\left[\frac{A}{\beta^4} - \frac{2b^2\alpha_1^2 k_{11}}{\pi^2\beta^2}(B + 2F) + \frac{\alpha_1^4 b^4}{\pi^4} D\right] \tag{111}$$

Comparing equations (110) and (111) gives

$$\left.\begin{aligned} \frac{2b^2\alpha_1^2 k_{11}}{\pi^2} &= -p \\ \frac{\alpha_1^4 b^4}{\pi^4} &= q \end{aligned}\right\} \tag{112}$$

so that equations (106) and (107) become

$$\left.\begin{aligned} C_{1x} &= \frac{\pi^4}{b^4} E_s I_s \left\{ \left(A + \mu \frac{E_{tc}}{E_c} \right) \frac{1}{\beta^4} + \frac{p}{2\beta^2} \left[F + (B + F) \frac{\theta_y}{\theta_x} \right] \right\} \\ C_{1y} &= \frac{\pi^4}{b^4} E_s I_s \left\{ qD + \frac{p}{2\beta^2} \left[F + (B + F) \frac{\theta_x}{\theta_y} \right] \right\} \end{aligned}\right\} \tag{113}$$

For example, for clamped edges, from table 1 of reference 11, $p = 2.5$ and $q = 5$. From references 35 and 36 for these boundary conditions, $\alpha_1 = 2.365/c$, where $c = b/2$ so that $\alpha_1 b = 4.73$. Further, $k_{11} = -0.54984$. With these values

$$\left.\begin{aligned} \frac{2b^2 \alpha_1^2 k_{11}}{\pi^2} &= -2.5 \\ \frac{\alpha_1^4 b^4}{\pi^4} &= 5.15 \end{aligned}\right\} \tag{114}$$

which is in excellent agreement with the more accurate values $-p = -2.5$ and $q = 5$ from equation (112).

Defining, as in reference 31, the shear stiffness D_{Q_x} as the ratio of shear to shear angle or

$$\left.\begin{aligned} D_{Q_x} &= Q_x/\gamma_x \\ D_{Q_y} &= Q_y/\gamma_y \end{aligned}\right\} \tag{115}$$

In case 2

$$\left.\begin{aligned} Q_{2x} &= D_{Q_x} \gamma_x = D_{Q_x} \frac{\partial w_{2x}}{\partial x} \\ Q_{2y} &= D_{Q_y} \gamma_y = D_{Q_y} \frac{\partial w_{2y}}{\partial y} \end{aligned}\right\} \tag{116}$$

where D_{Q_x} and D_{Q_y} are given in reference 38. This gives, analogous to equation (68),

$$\left.\begin{aligned} C_{2x} &= \frac{R_{2x}}{w_{2x}} = -\frac{1}{w_{2x}}\frac{\partial Q_{2x}}{\partial x} = -\frac{D_{Q_x}}{w_{2x}}\frac{\partial^2 w_{2x}}{\partial x^2} \\ C_{2y} &= -\frac{D_{Q_y}}{w_{2y}}\frac{\partial^2 w_{2y}}{\partial y^2} \end{aligned}\right\} \tag{117}$$

Using equation (69) this becomes

$$\left.\begin{aligned} C_{2x} &= \frac{\pi^2}{a^2} D_{Q_x} \\ C_{2y} &= \frac{\pi^2}{b^2} D_{Q_y} \end{aligned}\right\} \tag{118}$$

Insertion of the first equations in equations (113) and (118) into equation (75) yields

$$\theta_x = \frac{1}{1 + \bar{r}_x\left\{\left(A + \mu\frac{E_{tc}}{E_c}\right)\frac{1}{\beta^2} + \frac{p}{2}\left[F + (B + F)\frac{\theta_y}{\theta_x}\right]\right\}} \tag{119}$$

where

$$\bar{r}_x = \frac{\pi^2 E_s I_s}{b^2 D_{Q_x}} \tag{120}$$

from which

$$\left\{1 + \left[\left(A + \mu\frac{E_{tc}}{E_c}\right)\frac{1}{\beta^2} + \frac{p}{2}F\right]\bar{r}_x\right\}\theta_x + \frac{p}{2}(B + F)\bar{r}_x\theta_y = 1 \tag{121}$$

From equation (76) and the second equations in equations (113) and (118)

$$\theta_y = \frac{1}{1 + \bar{r}_y \left\{ qD + \frac{p}{2\beta^2} \left[F + (B + F) \frac{\theta_x}{\theta_y} \right] \right\}} \tag{122}$$

where

$$\bar{r}_y = \frac{\pi^2 E_s I_s}{b^2 D_{Q_y}} \tag{123}$$

From equation (122)

$$\frac{p}{2} (B + F) \bar{r}_y \theta_x + \left[\beta^2 + \left(qD\beta^2 + \frac{p}{2} F \right) \bar{r}_y \right] \theta_y = \beta^2 \tag{124}$$

Equations (121) and (124) yield

$$\left.\begin{aligned} \theta_x &= \frac{\beta^2 + \left(qD\beta^2 + \frac{p}{2} F \right) \bar{r}_y - \frac{p}{2} (B + F) \beta^2 \bar{r}_x}{\left[1 + \left(\frac{A + \left(\mu E_{tc}/E \right)}{\beta^2} + \frac{p}{2} F \right) \bar{r}_x \right] \left[\beta^2 + \left(qD\beta^2 + \frac{p}{2} F \right) \bar{r}_y \right] - \frac{p^2}{4} (B + F)^2 \bar{r}_x \bar{r}_y} \\ \theta_y &= \frac{\left[1 + \left(\frac{A + \mu E_{tc}/E_c}{\beta^2} + \frac{p}{2} F \right) \bar{r}_x \right] \beta^2 - \frac{p}{2} (B + F) \bar{r}_y}{\left[1 + \left(\frac{A + \mu E_{tc}/E}{\beta^2} + \frac{p}{2} F \right) \bar{r}_x \right] \left[\beta^2 + \left(qD\beta^2 + \frac{p}{2} F \right) \bar{r}_y \right] - \frac{p^2}{4} (B + F)^2 \bar{r}_x \bar{r}_y} \end{aligned}\right\} \tag{125}$$

In connection with equation (100), equations (85), (86), and (87) apply here as well, so that equation (2) becomes, analogous to equation (88),

$$P_{cr} = P_0 + \frac{a^2}{\pi^2} \left(\theta_x C_{1x} + \theta_y C_{1y} \right) \tag{126}$$

where P_0 can usually be neglected. For simply supported plates, from references 11 and 12,

$$P_0 = \frac{2\pi^2 E_s I_f}{b^2}\left[\frac{A}{\beta^2} + 2(B + 2F) + D\beta^2\right] \tag{127}$$

where (fig. 3)

$$I_f = h^3/12 \tag{128}$$

For clamped plates the deflections w_{1y} and w_{2y} of the Y-strips are shown in figure 15. Hence only for the deflection w_{1y} do the faces act as clamped, while with the deflection w_{2y} they practically act as simply supported so that in accordance with item (5) in the section "Description of Method"

$$P_0 = \frac{w_{1ym}}{w_m} P_{01} + \frac{w_{2ym}}{w_m} P_{02} = \theta_y P_{01} + \left(1 - \theta_y\right) P_{02} \tag{129}$$

where P_{02} is identical to P_0 from equation (127) and, since the clamped edges $p = 2.5$ and $q = 5$ (refs. 11 and 12),

$$P_{01} = \frac{2\pi^2 E_s I_f}{b^2}\left[\frac{A}{\beta^2} + 2.5(B + 2F) + 5D\beta^2\right] \tag{130}$$

Equation (129) is slightly conservative, since for case 2 the break in the faces at $y = 0$ and b requires extra energy. Hence, for simply supported unloaded edges, from equation (126) using equations (113) and (127) with $p = 2$ and $q = 1$,

$$P_{cr} = \frac{2\pi^2 E_s I_f}{b^2}\left[\frac{A}{\beta^2} + 2(B + 2F) + D\beta^2\right] +$$

$$\frac{\pi^2 E_s I_s}{b^2}\left\{\left[\frac{A + \left(\mu E_{tc}/E\right)}{\beta^2} + (B + 2F)\right]\theta_x + \left[(B + 2F) + D\beta^2\right]\theta_y\right\} \tag{131}$$

For clamped sandwich plates, from equations (113), (126), (127), (129), and (130), with $p = 2.5$ and $q = 5$,

$$P_{cr} = \frac{2\pi^2 E_s I_f}{b^2}\left[\frac{A}{\beta^2} + \left(2 + \frac{1}{2}\theta_y\right)(B + 2F) + \left(1 + 4\theta_y\right)D\beta^2\right] +$$

$$\frac{\pi^2 E_s I_s}{b^2}\left\{\left[\frac{A + \left(\mu E_{tc}/E_c\right)}{\beta^2} + 1.25(B + 2F)\right]\theta_x + \left[1.25(B + 2F) + 5D\beta^2\right]\theta_y\right\} \tag{132}$$

where θ_x and θ_y are given by equation (125). Besides from the formulas in references 33 and 34 A, B, D, and F can be read directly from charts in reference 39 as functions of the secant and tangent moduli for the actual buckling stress $\sigma_{cr} = P_{cr}/2h$.

In the elastic range, from references 33 or 34,

$$A = B + 2F = D = 1\Big/\left(1 - \nu^2\right) \tag{133}$$

so that for a simply supported plate equation (131) reduces to

$$P_{cr} = \frac{2\pi^2 E_s I_f}{\left(1 - \nu^2\right)b^2}\left(\frac{1}{\beta} + \beta\right)^2 + \frac{\pi^2 E_s I_s}{\left(1 - \nu^2\right)b^2}\left\{\left[\frac{1 + \left(1 - \nu^2\right)\mu}{\beta^2} + 1\right]\theta_x + \left(1 + \beta^2\right)\theta_y\right\} \tag{134}$$

where θ_x and θ_y from equation (125) with $p = 2$ and $q = 1$ reduce to

$$\left.\begin{aligned}
\theta_x &= \frac{\beta^2 + \frac{\beta^2 + \frac{1}{2}(1-\nu)}{1-\nu^2}\bar{r}_y - \frac{\beta^2}{2(1-\nu)}\bar{r}_x}{\left\{1 + \left[\frac{1 + (1-\nu^2)\mu}{\beta^2} + \frac{1-\nu}{2}\right]\frac{\bar{r}_x}{1-\nu^2}\right\}\left[\beta^2 + \left(\beta^2 + \frac{1-\nu}{2}\right)\frac{\bar{r}_y}{1-\nu^2}\right] - \frac{\bar{r}_x\bar{r}_y}{4(1-\nu^2)}} \\
\theta_y &= \frac{\beta^2 + \left[\frac{1 - (1-\nu^2)\mu}{1-\nu^2} + \frac{\beta^2}{2(1+\nu)}\right]\bar{r}_x - \frac{1}{2(1-\nu)}\bar{r}_y}{\left[1 + \left(\frac{1 + (1-\nu^2)\mu}{\beta^2} + \frac{1-\nu}{2}\right)\frac{\bar{r}_x}{1-\nu^2}\right]\left[\beta^2 + \left(\beta^2 + \frac{1-\nu}{2}\right)\frac{\bar{r}_y}{1-\nu^2}\right] - \frac{\bar{r}_x\bar{r}_y}{4(1-\nu^2)}}
\end{aligned}\right\} \tag{135}$$

If the proper flexural rigidity of the faces is neglected $\left(I_f = 0\right)$ and P_{cr} is written in the form

$$P_{cr} = k_s \frac{\pi^2 E_s I_s}{b^2} \tag{136}$$

k_s from equation (136) can be shown to be identical to k_s from reference 32. With $\mu = 0$, since in equation (135) $\bar{r}_x = (1 - \nu^2)r_x$ and $\bar{r}_y = (1 - \nu^2)r_y$, these equations for θ_x, θ_y, and P_{cr} reduce to equations (83) and (89), so that also these equations are exact.

For a clamped sandwich plate in the elastic range equation (132) reduces to

$$P_{cr} = \frac{2\pi^2 E_s I_f}{(1-\nu^2)b^2}\left[\frac{1}{\beta^2} + 2 + \frac{1}{2}\theta_y + \left(1 + 4\theta_y\right)\beta^2\right] +$$

$$\frac{\pi^2 E_s I_s}{(1-\nu^2)b^2}\left\{\left[\frac{1 + (1-\nu^2)\mu}{\beta^2} + 1.25\right]\theta_x + \left(1.25 + 5\beta^2\right)\theta_y\right\} \tag{137}$$

where, with $p = 2.5$ and $q = 5$, from equation (125)

$$\left.\begin{aligned}
\theta_x &= \frac{\beta^2 + \frac{5\beta^2 + 0.625(1-\nu)}{1-\nu^2}\bar{r}_y - 0.625\frac{\beta^2}{1-\nu}\bar{r}_x}{\left\{1 + \left[\frac{1+(1-\nu^2)\mu}{\beta^2} + 0.625(1-\nu)\right]\frac{\bar{r}_x}{1-\nu^2}\right\}\left\{\beta^2 + \left[5\beta^2 + 0.625(1-\nu)\right]\frac{\bar{r}_y}{1-\nu^2}\right\} - \frac{6.25\bar{r}_x\bar{r}_y}{16(1-\nu^2)}} \\
\theta_y &= \frac{\beta^2 + \left[\frac{1+(1-\nu^2)\mu}{1-\nu^2} + 0.625\frac{\beta^2}{1+\nu}\right]\bar{r}_x - 0.625\frac{1}{1-\nu}\bar{r}_y}{\left\{1 + \left[\frac{1+(1-\nu^2)\mu}{\beta^2} + 0.625(1-\nu)\right]\frac{\bar{r}_x}{1-\nu^2}\right\}\left\{\beta^2 + \left[5\beta^2 + 0.625(1-\nu)\right]\frac{\bar{r}_y}{1-\nu^2}\right\} - \frac{6.25\bar{r}_x\bar{r}_y}{16(1-\nu^2)}}
\end{aligned}\right\} \quad (138)$$

For isotropic core, $\bar{r}_x = \bar{r}_y = (1-\nu^2)r$ where r is given by equation (78) or (81) with $G_x = G_y = G_c$ or

$$r = \frac{\pi^2 E_s I_s}{(1-\nu^2)b^2 G_c (t+h)^2} \quad (139)$$

Here G_c is the modulus of rigidity of the core. Further $\mu = 0$. Thus equations (137) and (138) reduce to

$$P_{cr} = \frac{2\pi^2 E_s I_f}{(1-\nu^2)b^2}\left[\frac{1}{\beta^2} + 2 + \frac{1}{2}\theta_y + (1+4\theta_y)\beta^2\right] +$$

$$\frac{\pi^2 E_s I_s}{(1-\nu^2)b^2}\left[\left(\frac{1}{\beta^2} + 1.25\right)\theta_x + (1.25 + 5\beta^2)\theta_y\right] \quad (140)$$

where

$$\left.\begin{aligned}\theta_x &= \frac{\beta^2 + \left[3.75\beta^2 + 0.625(1-\nu)\left(1+\beta^2\right)\right]r}{\beta^2 + \left[1 + 5\beta^2 + 0.625(1-\nu)\left(1+\beta^2\right)\right]r + \left[3.4375 + 0.625(1-\nu)\left(\frac{1}{\beta^2} + 2.5 + 5\beta^2\right)\right]r^2} \\ \theta_y &= \frac{\beta^2 - \left[0.25 - 0.625(1-\nu)\left(1+\beta^2\right)\right]r}{\beta^2 + \left[1 + 5\beta^2 + 0.625(1-\nu)\left(1+\beta^2\right)\right]r + \left[3.4375 + 0.625(1-\nu)\left(\frac{1}{\beta^2} + 2.5 + 5\beta^2\right)\right]r^2}\end{aligned}\right\} \quad (141)$$

It seems that the maximum discrepancy between the simple formulas for isotropic-core sandwich plates derived in reference 11 and the exact calculation occurs for the present case of clamped edges. From reference 28 both lead to the same buckling loads for $r = 0$ and $r \geq 1$ and the maximum discrepancy of 7 percent occurs if r is about 0.25. From table 1 of reference 28 where, as usually can be done, the proper rigidities of the faces have been neglected, a minimum value of the buckling stress coefficient

$$k = \frac{b^2 P_{cr}}{\pi^2 N_s} = \frac{\left(1-\nu^2\right) b^2 P_{cr}}{\pi^2 E_s I_s} \quad (142)$$

occurs with $r = 0.25$ for $\beta = 0.6$ where $k = 2.88$, while from reference 11 for the same case $k = 3.08$. Also equations (140) and (141) with $I_f = 0$ for $r = 0$ and $r \geq 1$ lead to the same values of k as these given in reference 28. For the case of greatest discrepancy between references 11 and 28, with $r = 0.25$, $\beta = 0.6$, and $\nu = 0.333$, they yield $\theta_x = 0.524$, $\theta_y = 0.274$, and $k = 2.94$, or only 2 percent more than the exact k value from reference 28. On the other hand, though more accurate, equations (140) and (141) are more intricate than the equations derived in reference 11. Their advantage with respect to those in reference 28 is that an explicit formula is obtained for P_{cr} or k.

For sandwich plates with orthotropic core, where as stated in reference 14 the method of references 11 and 12 cannot be used if the ratio G_y/G_x differs too much from 1, the present formulas lead to very accurate results. It was shown in the foregoing discussion that for simply supported plates they are exact. For clamped plates, in the limiting case where $r_x = 0$ and with $\mu = 0$ and $I_f = 0$, equations (137) and (138) reduce to

$$P_{cr} = \frac{\pi^2 E_s I_s}{(1 - \nu^2)b^2}\left[\left(\frac{1}{\beta^2} + 1.25\right)\theta_x + \left(1.25 + 5\beta^2\right)\theta_y\right] \tag{143}$$

$$\left.\begin{aligned} \theta_x &= 1 \\ \theta_y &= \frac{\beta^2 - \left[0.625\bar{r}_y/(1 - \nu)\right]}{\beta^2 + \left\{\left[5\beta^2 + 0.625(1 - \nu)\right]\bar{r}_y/\left(1 - \nu^2\right)\right\}} \end{aligned}\right\} \tag{144}$$

From these formulas, for example, with $\beta = 1$, $\bar{r}_y = 0.25$, 1, and ∞, and $\nu = 0.33$, one finds that

$$k_s = \frac{b^2 P_{cr}}{\pi^2 E_s I_s} \tag{145}$$

is equal to 4.67, 2.59, and 1.45, respectively. From figure 4(a) of reference 32 for $\beta = 1$ and the same values of $\bar{r}_y$, k_s is 4.55, 2.51, and 1.40, respectively, so that the discrepancies are not more than 3 percent.

This shows that also for sandwich plates with orthotropic core the method of split rigidities leads to accurate results. If necessary, similar formulas can be derived for other boundary conditions.

Buckling of Homogeneous Plates Under Nonhomogeneous Stress Distribution

Item (6) in the section "Description of Method" can be used to calculate deflections of columns and plates with initial crookedness, as was done in footnote 2 of reference 1 and in reference 15, respectively. It can also be used to find the axial resistance of initially flat plates under nonhomogeneous stress distribution, as was done in references 15 and 17 for plates in the postbuckling stage. The same method can be applied for calculating the critical load for incipient buckling of plates under initially nonhomogeneous stresses. In all cases the restraining or internal action of the plate is derived from the case of uniformly

distributed stress. Hence the condition for the accuracy of this method is that the shape of the deflection surface for the nonhomogeneous stress distribution considered is practically similar to that under uniform stress.

Such a case occurs, for example, with buckling of a long simply supported flange under linearly distributed stresses σ_x (fig. 16). In a similar way as under uniform stresses σ_x the bending moments M_y (and M_x) will be relatively very small so that the plate can be assumed to remain straight in the lateral direction or

$$w = Ky \sin \frac{\pi}{a} x \tag{146}$$

For uniformly distributed compressive stress with Poisson's ratio equal to 0.3, from reference 40

$$\sigma_{cr} = k \frac{\pi^2 N}{b^2 t} = 0.425 \frac{\pi^2 N}{b^2 t} \tag{147}$$

The external and internal actions that are compared (item (2)) are the moments of the deflecting and restraining forces with respect to the hinged edge. For uniform compression the deflecting forces acting upon a small element $t\ dx\ dy$ are $-t\sigma_{cr}\left(\partial^2 w/\partial x^2\right) dx\ dy$, so that from equation (146) they can be expressed as

$$D = C_1 \sigma_{cr} w\ dx\ dy = C\sigma_{cr} y\ dy \tag{148}$$

where C is independent of y. Hence the external moment exerted by the forces D acting upon a cross strip $b\ dx$ about the hinged edge $y = 0$ is

$$M_{eu} = \int_0^b Dy\ dy = C\sigma_{cr} \int_0^b y^2\ dy = \frac{1}{3} C\sigma_{cr} b^3 \tag{149}$$

Then, from item (6), the moment exerted about the hinged edge by the restraining forces acting upon the strip must be

$$M_i = M_{eu} = \frac{1}{3} C\sigma_{cr} b^3 \tag{150}$$

Since under nonuniform compressive stresses (fig. 16) equation (146) remains valid, also in that case M_i is given by equation (150). With compressive stresses

$$\sigma_x = \sigma_e\left(1 - \tau \frac{b - y}{b}\right) \tag{151}$$

the deflecting forces are, analogous to equation (148), $D = C\sigma_x y\, dy$, so that they exert a moment about the hinged edge of

$$M_e = \int_0^b Dy\, dy = C\int_0^b \sigma_x y^2\, dy = C\sigma_e\left[(1 - \tau)\int_0^b y^2\, dy + \frac{\tau}{b}\int_0^b y^3\, dy\right]$$

$$= \frac{4 - \tau}{12} C\sigma_e b^3 \tag{152}$$

Since M_e should be equal to M_i, from equations (147), (150), and (152) the critical maximum edge stress σ_e is

$$(\sigma_e)_{cr} = \frac{4}{4 - \tau}\sigma_{cr} = \frac{1.70}{4 - \tau}\frac{\pi^2 N}{b^2 t} \tag{153}$$

For $\tau = 1$ and 2 this yields k values of 0.568 and 0.850, respectively, in accordance with values given in reference 40. If the maximum stress σ_e occurs at the hinged edge (fig. 17), so that

$$\sigma_x = \sigma_e\left(1 - \tau \frac{y}{b}\right) \tag{154}$$

and τ varies between 0 and 1, the external moment is

$$M_e = C\int_0^b \sigma_x y^2\, dy = C\sigma_e\left[\int_0^b y^2\, dy - \frac{\tau}{b}\int_0^b y^3\, dy\right] = \frac{4 - 3\tau}{12} C\sigma_e b^3 \tag{155}$$

so that from equations (147), (150), and (155)

$$(\sigma_e)_{cr} = \frac{4}{4 - 3\tau}\sigma_{cr} = \frac{1.70}{4 - 3\tau}\frac{\pi^2 N}{b^2 t} \tag{156}$$

For $\tau = 1$ one obtains $k = 1.70$, in accordance with reference 40.

Ultimate Load of Plates Under Compression

In reference 15 item (6) (section "Description of Method") was used for determining the postbuckling behavior of a simply supported plate, the unloaded edges of which are held straight in the plane of the plate, assuming the plate to remain elastic. This method will here be extended to the plastic range in order to find the ultimate load of such a plate (ref. 41).

It was shown in reference 15 that up to deflections of the order of the plate thickness t practical exact results can be obtained by assuming the shape of the deflection surface of the plate to remain similar to that at incipient buckling, that is,

$$w = w_m \sin\frac{\pi}{a}x \sin\frac{\pi}{b}y \tag{157}$$

where $a = b$. Considering the deflection to be developed in a Fourier series, the distribution of the total direct stress σ_x in the postbuckling range, as sketched in figure 18, will tend to superimpose on the deflection from equation (157) partial deflections $\Delta w = w_{13} \sin\frac{\pi}{a}x \sin\frac{3\pi}{b}y$, for which the individual equally distributed buckling stress σ_x is 25 times that for the mode of equation (157). The stresses σ_y (fig. 18) superimpose deflections $w_{31} \sin\frac{3\pi}{a}x \sin\frac{\pi}{b}y$ and $w_{33} \sin\frac{3\pi}{a}x \sin\frac{3\pi}{b}y$, with individual equally distributed buckling stresses σ_y that are 25 and 9 times, respectively, those connected with equation (157). Hence the required deflecting forces for bending in these modes are much higher than for bending in the mode of equation (157), which makes the contribution of these modes relatively small. In the elastic range the membrane stresses σ_{mx} and σ_{my} in figure 18 are (ref. 15)

$$\left.\begin{aligned} \sigma_{mx} &= \sigma_{mxm} \sin^2 \frac{\pi}{b} y \\ \sigma_{my} &= \sigma_{mym} \sin^2 \frac{\pi}{a} x \end{aligned}\right\} \tag{158}$$

In reference 41 it was shown that it is sufficiently accurate to assume the same distribution in the plastic range. Using a method that differs somewhat from that used in reference 15 the uniform stress distribution $(\sigma_x)_u$ that is equivalent to the membrane stresses σ_{mx} can be calculated as follows: If $\sigma_x = (\sigma_x)_u$ does not vary with y the work done by these compressive stresses per buckle with deflections w is from equation (157)

$$V_{xu} = \frac{t}{2}\int_0^a \int_0^b (\sigma_x)_u \left(\frac{\partial w}{\partial x}\right)^2 dx\, dy = \frac{t}{2} (\sigma_x)_u \frac{\pi^2}{a^2} w_m{}^2 \frac{ab}{4} \tag{159}$$

On the other hand the tensile stresses σ_{mx} from equation (158) would exert a work

$$V_{xm} = -\frac{t}{2}\int_0^a \int_0^b \sigma_{mxm} \sin^2 \frac{\pi}{b} y \left(\frac{\partial w}{\partial x}\right)^2 dx\, dy = -\frac{t}{2} \sigma_{mxm} \frac{\pi^2}{a^2} w_m{}^2 \frac{3}{16} ab \tag{160}$$

From equations (159) and (160) the membrane stresses σ_{mx} are equivalent to equally distributed compressive stresses

$$(\sigma_x)_u = -\frac{3}{4} \sigma_{mxm} \tag{161}$$

The work done by uniform compressive stresses $(\sigma_y)_u$ is

$$V_{yu} = \frac{t}{2}\int_0^a \int_0^b (\sigma_y)_u \left(\frac{\partial w}{\partial y}\right)^2 dx\, dy = \frac{t}{2} (\sigma_y)_u \frac{\pi^2}{b^2} w_m{}^2 \frac{ab}{4} \tag{162}$$

so that from equations (159) and (162) an equally distributed stress σ_y is equivalent to a stress

$$(\sigma_x)_u = \frac{a^2}{b^2}(\sigma_y)_u = \beta^2(\sigma_y)_u \tag{163}$$

Hence, from equations (161) and (163) the total load on the plate as shown in figure 18 is equivalent to a uniform load

$$(\sigma_x)_u = \sigma_{xe} - \frac{3}{4}\sigma_{mxm} + \beta^2\left(\frac{1}{2}\sigma_{mym} - \frac{3}{4}\sigma_{mym}\right) \tag{164}$$

The membrane stresses σ_{mxm} are caused by the increase in length of the middle strips GH due to the deflection w which amounts to

$$\delta = \frac{1}{2}\int_0^a \left(\frac{\partial w}{\partial x}\right)^2 dx = \frac{\pi^2}{4a} w_m^2 \tag{165}$$

so that the difference between the average direct strains in the strips AD and GH is

$$\epsilon_{xm} = \frac{\delta}{a} = \frac{\pi^2}{4}\left(\frac{w_m}{a}\right)^2 \tag{166}$$

Assuming, as proved to be true in the elastic range (ref. 15), that σ_x does not vary with x and that Poisson's ratio does not influence the stress distribution so that it can be assumed to be zero, this gives a stress

$$\sigma_{mxm} = E_{sx}\epsilon_{xm} = \frac{\pi^2}{4} E_{sx}\left(\frac{w_m}{a}\right)^2 \tag{167}$$

where E_{sx} is the secant modulus to be applied. Similarly

$$\sigma_{mym} = E_{sy}\epsilon_{ym} = \frac{\pi^2}{4} E_{sy}\left(\frac{w_m}{b}\right)^2 \tag{168}$$

so that

$$\sigma_{mym} = \beta^2 \frac{E_{sy}}{E_{sx}} \sigma_{mxm} \tag{169}$$

At incipient buckling the restraining forces offered by the bending rigidity of the plate are just in equilibrium with the deflecting forces caused by the compressive stresses $\sigma_x = \eta\sigma_{cr}$, where σ_{cr} is the elastic buckling stress of a simply supported plate (ref. 26, p. 329)

$$\sigma_{cr} = \left(\beta + \frac{1}{\beta}\right)^2 \frac{\pi^2 N}{b^2 t} = 0.905\left(\beta + \frac{1}{\beta}\right)^2 E\left(\frac{t}{b}\right)^2 \tag{170}$$

and η is the plastic reduction factor. The deflecting forces are proportional to the center deflection w_m of the plate. Since the restraining forces are due only to the bending stresses in the plate (the membrane forces are included in the loadings σ_x and σ_y) in the elastic range they are also proportional to the deflection w_m. Therefore, with finite deflections the plate will be able to resist stresses σ_x and σ_y (including the membrane stresses) that are equivalent to uniform stresses

$$(\sigma_x)_u = \bar{\eta}\sigma_{cr} \tag{171}$$

where $\bar{\eta}$ is the plastic reduction factor of the plate flexural rigidity at the actual finite deflection w_m. Since the actual loading of the plate is equivalent to $(\sigma_x)_u$ from equation (164), combination of equations (164), (169), and (171) gives

$$\sigma_{xe} - \frac{3}{4}\sigma_{mxm} - \frac{1}{4}\beta^4 \frac{E_{sy}}{E_{sx}} \sigma_{mxm} = \bar{\eta}\sigma_{cr} \tag{172}$$

or

$$\sigma_{mxm} = \frac{4(\sigma_{xe} - \bar{\eta}\sigma_{cr})}{3 + \left(\beta^4 E_{sy}/E_{sx}\right)} \tag{173}$$

Hence from figure 18 and equation (158) the average stress, that is, the postbuckling stress σ_{xp}, is

$$\sigma_{xp} = \sigma_{xe} - \int_0^b \sigma_{mx}\, dy = \sigma_{xe} - \frac{1}{2}\sigma_{mxm} \tag{174}$$

Apparently the postbuckling stress σ_{xp} depends on $\beta = a/b$. In general, the value of β corresponding to a minimum value of σ_{xp} will decrease as the deflection w_m increases. However, as explained in reference 41, the plate will not be free to change its wave length continuously because at a certain wave length the buckles will "freeze." This process can be illustrated by considering a very long plate for which any wave length would satisfy the boundary conditions. For such a plate the plastic deformation due to compressive and bending stresses will cause permanent buckles so that after a certain stress has been reached the wave length becomes fixed. From available test results it appears that the wave length that establishes itself at incipient buckling is maintained in the postbuckling range. The only plates that exhibit a postbuckling stress are those that buckle in the elastic range, where at incipient buckling $\beta = a/b = 1$. Hence in equation (173) β may be assumed to be 1. In that case E_{sy}/E_{sx} may also be assumed to be 1.

From references 25 and 42 for simply supported plates with edges that are not held straight the ultimate load is a function of the yield stress σ_{ys} and the critical stress σ_{cr}. The (average) ultimate stress was found experimentally as

$$\sigma_{ult} = \left(b_e/b\right)\sigma_{ys} = \sqrt{\sigma_{cr}\sigma_{ys}} - 0.25\sigma_{cr} \tag{175}$$

Assuming that in the present case, where the edges are held straight, the ultimate load is reached when the edge stresses σ_{xe} reach the yield stress, from equation (173) with $\beta = E_{sy}/E_{sx} = 1$ and $\sigma_{xe} = \sigma_{ys}$,

$$\sigma_{mxm} = \sigma_{ys} - \bar{\eta}\sigma_{cr} \tag{176}$$

so that the ultimate stress is, from equation (174) with $\sigma_{xp} = \sigma_{ult}$ and $\sigma_{xe} = \sigma_{ys}$,

$$\sigma_{ult} = \sigma_{ys} - \frac{1}{2}\sigma_{mxm} \tag{177}$$

In reference 41 it was shown how for a given case $\bar{\eta}$ can be calculated from the plastic deformations of the plate. Since this calculation is very involved a direct formula was derived for $\bar{\eta}$, which for the case considered was shown to be in excellent agreement with the more exact calculation. From reference 17 for edges that are not held straight in the plane of the plate, to which equation (175) refers, the membrane stresses σ_{mx} and σ_{my} are equivalent to a uniform stress

$$(\sigma_x)_u = -0.848\sigma_{mxm} \tag{178}$$

Also in that case the equivalent loading of the plate should be equal to $\bar{\eta}\sigma_{cr}$. With edge stresses σ_{ys} this gives

$$\sigma_{ys} - 0.848\sigma_{mxm} = \bar{\eta}\sigma_{cr} \tag{179}$$

or

$$\sigma_{mxm} = 1.18\sigma_{ys} - 1.18\bar{\eta}\sigma_{cr} \tag{180}$$

Equation (174) also applies here so that, with $\sigma_{xp} = \sigma_{ult}$ and $\sigma_{xe} = \sigma_{ys}$, using equation (180) gives

$$\sigma_{ult} = \sigma_{ys} - \frac{1}{2}\sigma_{mxm} = 0.41\sigma_{ys} + 0.59\bar{\eta}\sigma_{cr} \tag{181}$$

and

$$\bar{\eta} = 1.7\frac{\sigma_{ult}}{\sigma_{cr}} - 0.7\frac{\sigma_{ys}}{\sigma_{cr}} \tag{182}$$

Insertion of σ_{ult} from equation (175) yields

$$\bar{\eta} = 1.7\left(\frac{\sigma_{ys}}{\sigma_{cr}}\right)^{\frac{1}{2}} - 0.425 - 0.7\frac{\sigma_{ys}}{\sigma_{cr}} \tag{183}$$

Since $\bar{\eta}$ thus is based on test results for relatively large deflections, it automatically also contains a correction on the use of equation (157) in that range. In order to apply this result to the present case with edges that are held straight, it should first be determined on which variables $\bar{\eta}$ depends. It is dependent on the direct stresses σ_x and σ_y

that vary with σ_{mxm} (fig. 18) and on the bending strains measured by the strain difference between both faces of the plate. At the center of the buckle this difference is

$$\Delta\epsilon_{xb} = -t\frac{\partial^2 w}{\partial x^2} = \frac{\pi^2}{a^2} w_m t \tag{184}$$

On the other hand, from equation (166),

$$w_m = \frac{2a}{\pi}\left(\epsilon_{xm}\right)^{1/2} = \frac{2a}{\pi}\left(\frac{\sigma_{mxm}}{E_{sx}}\right)^{1/2} \tag{185}$$

so that from equation (184), with $a = b$,

$$\Delta\epsilon_{xb} = \frac{2\pi t}{b}\left(\frac{\sigma_{mxm}}{E_{sx}}\right)^{1/2} \tag{186}$$

From equation (170), with $\beta = a/b = 1$,

$$\frac{t}{b} = 0.525\left(\frac{\sigma_{cr}}{E}\right)^{1/2} \tag{187}$$

so that equation (186) becomes

$$\Delta\epsilon_{xb} = 3.3\left(\frac{\sigma_{cr}}{E}\frac{\sigma_{mxm}}{E_{sx}}\right)^{1/2} \tag{188}$$

Hence, since $\bar{\eta}$ depends on σ_{mxm} and $\Delta\epsilon_{xb}$, it obviously can be considered as a function of σ_{mxm} and σ_{cr}. From equation (179)

$$\frac{\sigma_{ys}}{\sigma_{cr}} = 0.848\frac{\sigma_{mxm}}{\sigma_{cr}} + \bar{\eta} \tag{189}$$

Inserting this into equation (183) gives $\bar{\eta}$ as a function of σ_{mxm} and σ_{cr}

$$\bar{\eta} = 0.25 - 0.35 \frac{\sigma_{mxm}}{\sigma_{cr}} + 0.71\left(\frac{\sigma_{mxm}}{\sigma_{cr}}\right)^{1/2} \tag{190}$$

With this value of $\bar{\eta}$ for the present case, from equation (176),

$$\frac{\sigma_{mxm}}{\sigma_{cr}} = \frac{\sigma_{ys}}{\sigma_{cr}} - 0.25 + 0.35 \frac{\sigma_{mxm}}{\sigma_{cr}} - 0.71\left(\frac{\sigma_{mxm}}{\sigma_{cr}}\right)^{1/2} \tag{191}$$

from which

$$\frac{\sigma_{mxm}}{\sigma_{cr}} = \left[-0.545 + \left(1.54 \frac{\sigma_{ys}}{\sigma_{cr}} - 0.0865\right)^{1/2}\right]^2 \tag{192}$$

After calculating σ_{mxm} from equation (192), σ_{ult} follows from equation (177).

In figure 19 σ_{ult}/σ_{cr} from equation (175) has been plotted as a function of σ_{cr}/σ_{ys} as the dashed curve ①. In the same figure pertinent test results for simply supported plates with edges that are not held straight in their plane are indicated by squares, as plotted from reference 43. The squares refer to square-tube tests by Needham (ref. 44) and the diamonds refer to V-groove tests by Anderson and Anderson (ref. 45) which are also shown in reference 43. This shows that formula (175), determined by Winter from tests with light-gage steel (ref. 42) involving plates that are not held straight in their plane, leads to excellent results. Hence, the formula for $\bar{\eta}$, derived from it and presented herein as equation (190), can be considered as well based. Therefore the combination of equations (177) and (192) can be expected to yield satisfactory results for plates with simply supported edges that are held straight in the plane of the plate. In figure 19 σ_{ult}/σ_{cr} from these equations has been plotted against σ_{cr}/σ_{ys} as the solid curve ②; the test results from Botman (ref. 46), as given in reference 43, are indicated by triangles. These tests were done with three-bay plates between knife edges so that the edges were not held completely straight. The test results should therefore be located between the curves ① and ②, which indeed occurs. The theoretical results from reference 43 for plates with edges held straight are indicated by circles. These are a little above curve ②. This may be because in reference 43 Poisson's ratio was assumed to be 0.5 for plastic as well as elastic deformations which increase the plate rigidity above its actual value. Hence equations (177) and (192) yield reliable results.

Formulas based on the same principles have been derived in reference 41 for the ultimate load of simply supported and clamped plates under the additional influence of thermal stresses. Also formulas were derived for the equally distributed stresses $(\sigma_x)_u$ and $(\sigma_y)_u$ that are equivalent to arbitrarily distributed thermal stresses σ_x and σ_y as far as critical as well as ultimate loads are concerned.

PROBLEMS WHERE COMPONENT CASES HAVE DIFFERENT BOUNDARY CONDITIONS

Problems where the component cases have different boundary conditions have been dealt with in references 13, 16, 17, 18, and 19. As pointed out under item (6) these problems lead to more intricate relations between P_{cr} and P_1, P_2, . . . P_n than those where the boundary conditions for all cases are the same. A simple example is the problem of determining the buckling stress of an I-section about its minor axis. The buckling deflection of the cross section is shown in figure 20(a) and is split into case 1, a deflection as a column without distortion of the cross section (fig. 20(b)) and case 2, a distortion of the cross section (fig. 20(c)). This problem was dealt with extensively in reference 13 where the deflecting and restraining forces were chosen as the external and internal actions. This method was sufficiently accurate because the decrease of the column buckling stress σ_1 (case 1) or plate buckling stress σ_2 (case 2) from the interaction of cases 1 and 2 was only a small fraction of the actual buckling stress.

Somewhat more accuracy can be obtained by comparing the work done by deflecting and that done by restraining forces. This method was used in references 17, 18, and 19. It will be demonstrated here in deriving the buckling stress of stringer panels.

The stringer panels considered are supported by stiffeners of equal cross section and located at equal distances b (fig. 21). The half wave length of buckling in the X-direction is denoted as a (fig. 22(b)). If no stiffeners were present, the buckling deflection of the plate would vary sinusoidally in the X- and Y-directions. If stiffeners are present and the deflection w_1 (fig. 22(a)) which determines the deflection of the stiffeners varies in the same way, the additional deflecting forces $-t\sigma_x(\partial^2 w/\partial x^2)$ per unit plate surface, caused by the additional compressive stresses σ_x which the panel can sustain due to the stiffeners, will as a whole vary sinusoidally too. Hence, equilibrium is possible if the restraining forces $EI(d^4w/dx^4)$ per unit length supplied by the

stiffeners also vary sinusoidally in both directions. This is indeed the case if w_1 varies sinusoidally. Hence, it may obviously be assumed that

$$w_1 = w_{1m} \sin \frac{\pi x}{a} \sin \frac{\pi y}{nb} = Y_1 \sin \lambda x \tag{193}$$

where

$$\lambda = \pi/a \tag{194}$$

In a similar way, as was done in reference 13 (fig. 20) for determining the interaction between column and plate buckling, the buckling deflection of the panel (fig. 22(a)) could now be split into two cases, and the buckling stress σ_{cr} expressed in terms of the individual buckling stresses for these cases. In the present case a slightly different approach is used by first splitting off the buckling stress σ_0 of the unstiffened sheet, caused by its buckling into the shape w_1 from equation (193) and denoted as case 0, as indicated by the first method under item (5). From page 329 of reference 26,

$$\sigma_0 = k_0 \frac{\pi^2 N}{b^2 t} = \left(\frac{a}{nb} + \frac{nb}{a}\right)^2 \frac{\pi^2 N}{n^2 b^2 t} = \left(\frac{\beta}{n^2} + \frac{1}{\beta}\right)^2 \frac{\pi^2 N}{b^2 t} \tag{195}$$

where

$$\beta = a/b \tag{196}$$

and N is the flexural rigidity of the sheet. The resulting buckling deflection of the reduced structure with buckling stress $\sigma_r = \sigma_{cr} - \sigma_0$, where consequently the partial buckling stress σ_0 caused by the rigidity of the sheet against bending into the shape w_1 is neglected, is then split into two individual cases. Case 1 is the deflection w_1, shown separately in figure 22(c). Case 2 is the extra deflection w_2, shown separately in figure 22(d), which is caused by the deflecting forces acting on the sheet and created by the partial buckling stresses $\sigma_r = \sigma_{cr} - \sigma_0$ that cannot be taken by the unstiffened sheet. These deflecting forces are consequently resisted by the stiffeners, which cause the bending of the sheet into shape w_2 like a laterally loaded continuous plate on several supports.

Hence, the actual buckling stress of the panel is

$$\sigma_{cr} = \sigma_0 + \sigma_r \tag{197}$$

where σ_r has to be expressed in the buckling stresses σ_1 and σ_2 for the individual cases 1 and 2, respectively.

Since the flexural rigidity of the sheet has to be neglected here, in case 1 the buckling stress σ_1 is due to the flexural rigidity of the stiffeners alone. The critical thrust of the single stiffeners, with effective moment of inertia I, is

$$P_1 = \pi^2 EI/a^2 = \lambda^2 EI \tag{198}$$

Hence, the restraining force R_1 acting on an element of length dx of a stiffener if bent into a half sine wave is equal to the deflecting force $D_1 = -P_1\left(\partial^2 w_1/\partial x^2\right) dx$ or, from equation (193),

$$R_1 = D_1 = \lambda^2 P_1 w_1 \, dx \tag{199}$$

At incipient buckling of the complete panel the compression $A_{st}\sigma_{cr}$ in the stiffener itself, with cross section A_{st}, causes a deflecting force

$$D_s = -A_{st}\sigma_{cr}\left(\partial^2 w_1/\partial x^2\right) dx = \lambda^2 A_{st}\sigma_{cr} w_1 \, dx \tag{200}$$

so that the restraining force exerted by a stiffener on the sheet is only

$$R_1' = R_1 - D_{st} = \lambda^2\left(P_1 - A_{st}\sigma_{cr}\right) w_1 \, dx \tag{201}$$

Therefore, by comparing equations (199) and (201), the restraining force exerted by a stiffener on the sheet is equal to that exerted by a stiffener with a zero cross section and a critical thrust

$$P_1' = P_1 - A_{st}\sigma_{cr} = \lambda^2 EI - A_{st}\sigma_{cr} \tag{202}$$

The buckling stress for buckling in a shape like that in figure 22(d) may be written in general as (ref. 25)

$$\sigma_2 = k_2 \frac{\pi^2 N}{b^2 t} = \left(\frac{1}{\beta^2} + p + q\beta^2 \right) \frac{\pi^2 N}{b^2 t} \tag{203}$$

where the computation for p and q is given in the appendix. However, since only the reduced case is considered, where the part σ_0 from equation (195) for buckling in a shape like w_1 must be ignored, the critical stress for the present case 2 is

$$\sigma_2' = \sigma_2 - \sigma_0 = k_2' \frac{\pi^2 N}{b^2 t} = \left[p - \frac{2}{n^2} + \left(q - \frac{1}{n^4} \right) \beta^2 \right] \frac{\pi^2 N}{b^2 t} \tag{204}$$

In order to express the reduced critical stress σ_r of the combined structure in terms of P_1' and σ_2' from equations (202) and (204), the work done by the deflecting and restraining forces will be compared. The deflections w_1 and w_2 in figure 22 both vary sinusoidally in the X-direction (fig. 22(b)) so that, similar to equation (193),

$$w_2 = Y_2 \sin \lambda x \tag{205}$$

where Y_2 is a function of y alone. Hence, at the reduced buckling stress the deflecting force in the Z-direction (fig. 22(a)) exerted on a sheet element $t\,dx\,dy$ as a consequence of the deflection $w = w_1 + w_2$ is $-t\sigma_r\left(\partial^2 w/\partial x^2\right) dx\,dy$ or, from equations (193) and (205),

$$D = \lambda^2 t \sigma_r \left(w_1 + w_2 \right) dx\,dy \tag{206}$$

Since from figure 22(a) the deflection w_2 does not involve any deflection of the stiffeners, it is evident that the work done by the deflecting forces for the deflection w_2 is taken entirely by bending of the sheet in the shape w_2. Furthermore, since the reduced case is considered, where the flexural rigidity of the sheet is ignored for the shape w_1, the work done by the deflecting forces for the deflection w_1 is taken by bending of the stiffeners alone.

The deflection w_1 will be considered first. Denoting the deflections of the stiffeners as

$$w_{st} = w_{stm} \sin \lambda x \tag{207}$$

where $w_{st} = w_1$, from equations (201) and (202) the restraining force exerted by a stiffener per length dx is

$$R_1' = \lambda^2 P_1' w_{st}\, dx \tag{208}$$

From the foregoing discussion the work done by the deflecting forces D from equation (206) for the deflection w_1 has to be equal to the total negative work done by the restraining forces R_1' from equation (208) furnished by the stiffeners. Hence,

$$\frac{1}{2}\iint D w_1\, dx\, dy = \frac{1}{2}\iint R_1' w_1\, dx\, dy$$

or, using equations (206) and (208) and dropping the terms $\lambda^2/2$,

$$t\sigma_r \iint w_1^2\, dx\, dy + t\sigma_r \iint w_1 w_2\, dx\, dy = P_1' \int \sum w_{st}^2\, dx \tag{209}$$

where the double integrals have to be extended over the entire sheet with dimensions a times nb and the summation sign refers to the $(n - 1)$ stiffeners. Equation (209) may be written in the form

$$nbt\sigma_r \left(w_{1m} + \varphi w_{2m}\right) = P_1' \psi w_{1m} \tag{210}$$

where w_{1m} and w_{2m} are indicated in figure 22(a) and where

$$\varphi = \frac{w_{1m}}{w_{2m}} \frac{\iint w_1 w_2\, dx\, dy}{\iint w_1^2\, dx\, dy} \tag{211}$$

and, since $w_{st} = w_1$ (fig. 22(a)), using equation (193) gives

$$\psi = \frac{nb \int \sum w_{st}^2\, dx}{\iint w_1^2\, dx\, dy} = \frac{nb \sum w_{st}^2}{\int_0^{nb} w_1^2\, dy} = \frac{nb \sum_{i=1}^{i=n-1} \sin^2 \frac{\pi}{nb}\, ib}{\int_0^{nb} \sin^2 \frac{\pi}{nb}\, y\, dy} = n \tag{212}$$

Hence equation (210) transforms to

$$\left(\sigma_r - \sigma_1'\right) w_{1m} + \varphi \sigma_r w_{2m} = 0 \tag{213}$$

where, from equation (202),

$$\sigma_1' = \frac{P_1'}{bt} = \sigma_1 - \kappa \sigma_{cr} \tag{214}$$

$$\sigma_1 = k_1 \frac{\pi^2 N}{b^2 t} = \frac{P_1}{bt} = \frac{\pi^2 EI}{a^2 bt} = \frac{1}{\beta^2} \frac{EI}{bN} \frac{\pi^2 N}{b^2 t} \tag{215}$$

$$\kappa = \frac{A_{st}}{bt} \tag{216}$$

Replacing σ_1' in equation (213) by the last term of equation (214), in which again σ_{cr} is expressed according to equation (197), equation (213) becomes

$$\left[(1 + \kappa)\sigma_r - \left(\sigma_1 - \kappa \sigma_0\right)\right] w_{1m} + \varphi \sigma_r w_{2m} = 0 \tag{217}$$

In order to obtain a second relation between w_{1m} and w_{2m} the work done for the deflection w_2 is considered. In case 2 buckling occurs at the stress σ_2' from equation (204), so that the restraining force R_2 acting on an element $t\ dx\ dy$ is equal to the deflecting force $D_2 = -t\sigma_2'\left(\partial^2 w_2 / \partial x^2\right) dx\ dy = \lambda^2 t \sigma_2' w_2\ dx\ dy$. This restraining force R_2 depends on the deflection w_2 alone and not on the compressive stress so that, with the assumption that in the combined case the deflection w_2 has the same shape as in case 2, also in the combined case the restraining force is

$$R_2 = \lambda^2 t \sigma_2' w_2\ dx\ dy \tag{218}$$

Equating the work done for the deflection w_2 by the deflecting forces D from equation (206) to the negative work done by the restraining forces R_2 from equation (218) gives

$$\frac{1}{2}\iint Dw_2 \, dx \, dy = \frac{1}{2}\iint R_2 w_2 \, dx \, dy$$

Using equations (206) and (218) and dropping the terms $\lambda^2/2$, this becomes

$$t\sigma_r \iint w_1 w_2 \, dx \, dy + t\sigma_r \iint w_2^2 \, dx \, dy = t\sigma_2' \iint w_2^2 \, dx \, dy \tag{219}$$

or

$$\gamma \sigma_r w_{1m} + \left(\sigma_r - \sigma_2'\right) w_{2m} = 0 \tag{220}$$

where

$$\gamma = \frac{w_{2m}}{w_{1m}} \frac{\iint w_1 w_2 \, dx \, dy}{\iint w_2^2 \, dx \, dy} \tag{221}$$

The buckling condition is obtained from the two homogeneous equations (217) and (220) by equating the denominator determinant to zero, which yields σ_r, so that from equation (197)

$$\sigma_{cr} = \sigma_0 + \sigma_r$$

$$= \sigma_0 + \frac{\sigma_1 - \kappa\sigma_0 + (1+\kappa)\sigma_2'}{2(1-\gamma\varphi+\kappa)} \left(1 - \left\{ 1 - \frac{4(1-\gamma\varphi+\kappa)\left(\sigma_1 - \kappa\sigma_0\right)\sigma_2'}{\left[\sigma_1 - \kappa\sigma_0 + (1+\kappa)\sigma_2'\right]^2} \right\}^{1/2} \right) \tag{222}$$

or

$$\sigma_{cr} = k_{cr} \frac{\pi^2 N}{b^2 t} \tag{223}$$

where

$$k_{cr} = k_0 + \frac{1 + \Omega(1 + \kappa)}{2(1 - \gamma\varphi + \kappa)} \left(k_1 - \kappa k_0\right)\left(1 - \left\{1 - \frac{4(1 - \gamma\varphi + \kappa)\Omega}{\left[1 + \Omega(1 + \kappa)\right]^2}\right\}^{1/2}\right) \tag{224}$$

$$\Omega = k_2' \Big/ \left(k_1 - \kappa k_0\right) \tag{225}$$

and from equations (195), (204), (215), and (216)

$$\left.\begin{aligned} k_0 &= \left(\frac{\beta}{n^2} + \frac{1}{\beta}\right)^2 \\ k_1 &= \frac{1}{\beta^2} \frac{EI}{bN} \\ k_2' &= p - \frac{2}{n^2} + \left(q - \frac{1}{n^4}\right)\beta^2 \\ \kappa &= \frac{A_{st}}{bt} \end{aligned}\right\} \tag{226}$$

The values of p, q, and $\gamma\varphi$ for the cases of 1, 2, 3, and an infinite number of stiffeners are determined in the appendix and are assembled in table 2. If $k_1 = 0$ and $\kappa = 0$ so that no stiffeners are present, equation (224) reduces to $k_{cr} = k_0$, as it should be. If k_2' and thus Ω are infinite, so that no interaction occurs, equation (224) becomes

$$k_{cr} = \frac{\left[\left(\frac{\beta}{n^2} + \frac{1}{\beta}\right)^2 + \frac{1}{\beta^2} \frac{EI}{bN}\right]}{(1 + \kappa)} \tag{227}$$

in accordance with equation (1) of reference 47. Equation (227) may be used if $\beta > 8$. The largest interaction occurs for small values of β. In table 3 the results from equation (224) for $\beta = 1$ are compared with those scaled from the graphs of reference 47. The values from reference 47 for $k_{cr} > 4$ refer to the extension of the $EI/(bN)$ curves. The only important discrepancies occur for $n = 3$, $EI/(bN) = 0$, and $\kappa = 0$, where the value from reference 47 is placed within parentheses, since here indeed from equations (224) and (226) $k_{cr} = k_0 = 100/81 = 1.235$ so that the graph seems to be inaccurate at that point.

The interaction is the smaller the larger the value of Ω is from equation (225). In a similar way as was done with equation (69) of reference 13, for not-too-small values of Ω equation (224) may be simplified by observing that the term in the large parentheses may be written as

$$1 - (1 - \epsilon)^{1/2} = 1 - \left(1 - \frac{1}{2}\epsilon - \frac{1}{8}\epsilon^2\right) = \frac{1}{2}\epsilon\left(1 + \frac{1}{4}\epsilon\right) \qquad (228)$$

since in that case ϵ is small with respect to unity so that equation (224) transforms to

$$k_{cr} = k_0 + \frac{\Omega}{1 + \Omega(1 + \kappa)}\left[1 + \frac{(1 - \gamma\varphi + \kappa)\Omega}{\left[1 + \Omega(1 + \kappa)\right]^2}\right](k_1 - \kappa k_0) \qquad (229)$$

For still larger values of Ω, the term 1 in the denominator of the fraction within the large brackets may be neglected, so that equation (229) becomes

$$k_{cr} = k_0 + \left[\Omega + \frac{1 - \gamma\varphi + \kappa}{(1 + \kappa)^2}\right]\frac{k_1 - \kappa k_0}{1 + \Omega(1 + \kappa)} \qquad (230)$$

Equations (229) and (230) are sufficiently accurate if Ω is larger than 1 and 4, respectively.

Values of k_{cr} may be calculated directly from equations (224), (229), or (230). They have to be calculated for half wave lengths $a = l/m$, where l is the simply supported length of the panel in the X-direction (fig. 1) and m is an integer (for only an infinite number of stiffeners can a be assumed to be equal to l). The lowest value of k_{cr} so obtained has to be inserted into equation (223). The effective moment of inertia I of the stiffeners to be used in

equations (226) for calculating k_1 has to be determined as shown in reference 20, where also a formula for the buckling stress coefficient for forced crippling is derived from equation (224).

This example shows that the method is applicable and gives accurate results for very intricate problems as is shown also by its application in references 13 and 17. The present problem was also worked out for stresses σ_y acting simultaneously in a direction perpendicular to the stringers as may be caused by thermal stresses, but it was thought that omission of the stresses σ_y gives a clearer picture of the method.

It should be noted that in reference 13, where the deflecting and restraining forces acting upon an arbitrary small element were chosen as the external and internal actions, these forces were expressed in terms of the maximum deflections w, w_1, and w_2 to which they were proportional. In the present case, and also in reference 17, where the work done by the deflecting and restraining forces was considered, the forces acting upon all elements must be taken into account. These forces cannot be expressed in terms of the maximum deflections, since for different elements different proportionality factors apply. Therefore they were expressed in terms of the local deflections w, w_1, and w_2 of the individual elements, which expression in all cases considered was facilitated by the sinusoidal variation of the deflections in the X-direction by which the deflecting forces $-t\sigma_x \partial^2 w/\partial x^2$ are proportional to w.

Since references 13 and 17, where the method was applied to several other cases with different boundary conditions of the component modes, are directly available, it is thought unnecessary to give other examples. The reader therefore is requested to consider references 13 and 17 as part of this section.

Cornell University,
Ithaca, N. Y., June 28, 1956.

APPENDIX

COMPUTATION OF p, q, AND $\gamma\Phi$

Computation of p and q in Equation (203)

For n = 2.- For plates with one stiffener (fig. 23(a)) in case 2 (fig. 22(d)) each plate of width b can be considered as simply supported at one unloaded side and clamped at the other one. From reference 48 for the clamped simply supported case $p = 2.27$ and $q = 2.45$.

For n = 3.- For plates with two stiffeners (fig. 23(b)) plate AB is simply supported at edge A while at B it is subjected to a moment that varies sinusoidally in the X-direction. Plate BC is subjected to equal and opposite sinusoidal moments at edges B and C. The buckling coefficient k_2 can be determined by requiring that the spring constant against rotation of plate AB along B is equal and opposite to that of BC along B. Spring constants for these cases or rather the specific angle rotations were derived in reference 49, where they are given by equations (48), (52), (53), and (54). The same results were obtained in reference 50 and are presented in tables in reference 51, where the stiffnesses S^{II} and S^{IV} are the quarter spring constants referring to the present plates AB and BC in B. Hence, k_2 is determined by the condition $S^{II} = -S^{IV}$. It appears that the minimum value of k_2 occurs for $\beta = a/b = 0.72$ and is equal to 6.15. From equation (6.4.1) of reference 25 this minimum is

$$(k_2)_{min} = p + 2\sqrt{q} \tag{A1}$$

Inserting the value 6.15 into equation (A1) and $k_2 = 6.935$, obtained for $\beta = 1$, into equation (203), one obtains $p = 2.36$ and $q = 3.58$.

For n = 4.- In the case of $n = 4$, (fig. 23(c)), from symmetry plate BC can be considered as clamped at edge C so that, with the notations of reference 51, the condition at B is $S^{II} = -S$, yielding a minimum value of $k_2 = 6.47$ and, for $\beta = 0.9$, $k_2 = 7.00$. From equations (A1) and (203) this results in values of $p = 2.37$ and $q = 4.20$.

For n = ∞.- For the case of $n = \infty$ all plates can be assumed to be clamped at both edges (fig. 23(d)) so that, from reference 25, $p = 2.5$ and $q = 5$. Values of p and q are assembled in table 2.

Computation of $\gamma\varphi$

From equations (211), (193), and (205),

$$\varphi = \frac{w_{1m}}{w_{2m}} \frac{\iint w_1 w_2 \, dx \, dy}{\iint w_1^2 \, dx \, dy} = \frac{w_{1m}}{w_{2m}} \frac{\int Y_1 Y_2 \, dy}{\int Y_1^2 \, dy} \tag{A2}$$

$$\gamma = \frac{w_{2m}}{w_{1m}} \frac{\iint w_1 w_2 \, dx \, dy}{\iint w_2^2 \, dx \, dy} = \frac{w_{2m}}{w_{1m}} \frac{\int Y_1 Y_2 \, dy}{\int Y_2^2 \, dy} \tag{A3}$$

From equation (193),

$$Y_1 = w_{1m} \sin \frac{\pi y}{nb} \tag{A4}$$

while from equation (624) of reference 25 for the plates considered, in general,

$$Y_2 = C_1 \cosh \alpha_1 y + C_2 \sinh \alpha_1 y + C_3 \cos \alpha_2 y + C_4 \sin \alpha_2 y \tag{A5}$$

where

$$\alpha_1, \alpha_2 = \left[\pm\lambda^2 + \lambda(t\sigma/N)^{1/2} \right]^{1/2} \tag{A6}$$

while λ is given by equation (194).

For $n = 2$.- Considering plate AB in figure 23(a), the conditions of simple support at $y = 0$ require that $C_1 = C_3 = 0$ so that from equation (A5)

$$Y_2 = C_2 \sin \alpha_1 y + C_4 \sin \alpha_2 y \tag{A7}$$

At $y = b$, $Y_2 = 0$ so that from equation (A7)

$$C_4 = -C_2 \frac{\sinh \alpha_1 b}{\sin \alpha_2 b} \tag{A8}$$

From table 26 of reference 25 the buckling coefficient k for plate AB in figure 23(a) (one edge, simply supported; the other, fixed) is 5.42, occurring for a half wave length $a = \beta b = 0.8b$ so that in equation (A6)

$$t\sigma/N = k\pi^2/b^2 = 5.42\pi^2/b^2$$

Hence, from equation (A6), with $\lambda = \pi/0.8b$, one obtains $\alpha_1 = 2.12\pi/b$ and $\alpha_2 = 1.165\pi/b$. Inserting this into equations (A7) and (A8)

$$Y_2 = C_2\left[\sinh (2.12\pi y/b) + 790 \sin (1.165\pi y/b)\right]$$

Denoting the deflection at $y = b/2$ as w_{2m}, this becomes

$$Y_2 = \frac{w_{2m}}{779}\left[\sinh (2.12\pi y/b) + 790 \sin (1.165\pi y/b)\right] \qquad (A9)$$

From equations (A4) and (A9) one obtains

$$\int_0^b Y_1^2 \, dy = 0.5bw_{1m}^2$$

$$\int_0^b Y_2^2 \, dy = 0.471bw_{2m}^2$$

$$\int_0^b Y_1 Y_2 \, dy = 0.366bw_{1m}w_{2m}$$

Hence, from equations (A2) and (A3) $\varphi = 0.732$, $\gamma = 0.778$, and $\gamma\varphi = 0.57$.

For $n = \infty$.- It is sufficiently accurate to calculate φ and γ for $n = 2$ and $n = \infty$ only and to derive from these values the values of φ and γ for intermediate n values. For infinite values of n (fig. 22(b))

$$Y_1 = w_{1m} = \text{Constant} \qquad (A10)$$

From symmetry (fig. 23(d)) equation (A5) transforms to

$$Y_2 = C_1 \cosh \alpha_1 y + C_3 \cos \alpha_2 y \qquad (A11)$$

At $y = b/2$, $Y_2 = 0$ so that from equation (A11)

$$C_3 = -C_1 \frac{\cosh(\alpha_1 b/2)}{\cos(\alpha_2 b/2)} \tag{A12}$$

From table 26 of reference 25 the buckling coefficient $k = 6.97$ occurs for $\beta = a/b = 0.668$, from which, in a way similar to that for $n = 2$, one obtains

$$\alpha_1 = 2.488\pi/b$$

$$\alpha_2 = 1.303\pi/b$$

and

$$Y_2 = \frac{w_{2m}}{55.5}\left[\cosh(2.488\pi y/b) + 54.5 \cos(1.303\pi y/b)\right] \tag{A13}$$

Hence, from equations (A10) and (A13)

$$\int_0^{b/2} Y_1^2 \, dy = 0.5bw_{1m}^2$$

$$\int_0^{b/2} Y_2^2 \, dy = 0.2065bw_{2m}^2$$

$$\int_0^{b/2} Y_1 Y_2 \, dy = w_{1m}\int_0^{b/2} Y_2 \, dy = 0.27bw_{1m}w_{2m}$$

so that from equations (A2) and (A3) $\varphi = 0.54$, $\gamma = 1.31$, and $\gamma\varphi = 0.707$.

For $n = 3$.- It is sufficiently accurate to consider the angle rotations at B and C (fig. 23(b)) to be zero so that the two outer plates AB and CD for $n = 3$ are similar to the plates for $n = 2$ (fig. 23(a) and the center plate is similar to those for infinite values of n (fig. 23(d)). Hence, as an average value

$$\gamma\varphi = \frac{1}{3}(0.57 + 0.707 + 0.57) = 0.616$$

For $n = 4$.- Assuming the angle rotations at B, C, and D to be zero (fig. 23(c)), one obtains, for $n = 4$,

$$\gamma\varphi = \frac{1}{2}(0.57 + 0.707) = 0.639$$

Values of $\gamma\varphi$ are assembled in table 2.

REFERENCES

1. Bijlaard, P. P.: Knikzekerheid van den bovenrand van open wandbruggen (Safety Against Buckling of the Top Chords of Pony Trusses). De Ingenieur (The Hague, Holland), Nr. 4, 1932.

2. Bijlaard, P. P.: Nauwkeurige berekening van de plooispanning van hoekstalen, zoowel voor bet elastische als voor bet plastische gebied (Accurate Computation of the Buckling Stress of the Legs of Steel Angles in the Elastic as Well as in the Plastic Range). De Ing. in Nederlandsch-Indië, Nr. 3, 1939, pp. 1.35-1.45.

3. Bijlaard, P. P.: Berekening van de knikspanning van gekoppelde profielen volgens een nieuwe methode (Computation of the Buckling Stress of Built-Up Sections Connected With Batten Plates by a New Method). De Ing. in Nederlandsch-Indië, Nr. 3, 1939, pp. 1.45-1.46.

4. Bijlaard, P. P.: On the Elastic Stability of Thin Plates, Supported by a Continuous Medium. Verh. Koninklijke Nederlandsche Akad. Wetenschappen, vol. XLIX, no. 10, 1946, pp. 1189-1199.

5. Bijlaard, P. P.: On the Elastic Stability of Sandwich Plates. Pts. I and II. Verh. Koninklijke Nederlandsche Akad. Wetenschappen, vol. L, nos. 1 and 2, 1947, pp. 79-87, 186-193.

6. Bijlaard, P. P.: Some Contributions to the Theory of Elastic and Plastic Stability. Pub. Int. Assoc. for Bridge and Structural Eng. (Zürich), vol. 8, 1947, pp. 17-80.

7. Bijlaard, P. P.: On the Torsional and Flexural Stability of Thin Walled Open Sections. Verh. Koninklijke Nederlandsche Akad. Wetenschappen, vol. LI, no. 3, 1948, pp. 314-321.

8. Bijlaard, P. P.: Stability of Sandwich Plates. Jour. Aero. Sci. (Readers' Forum), vol. 16, no. 9, Sept. 1949, pp. 573-574.

9. Bijlaard, P. P.: Analysis of the Elastic and Plastic Stability of Sandwich Plates by the Method of Split Rigidities. Preprint No. 259, Inst. Aero. Sci., Jan. 1950.

10. Bijlaard, P. P.: Stability of Sandwich Plates in Combined Shear and Compression. Jour. Aero. Sci. (Readers' Forum), vol. 17, no. 1, Jan. 1950, p. 63.

11. Bijlaard, P. P.: Analysis of the Elastic and Plastic Stability of Sandwich Plates by the Method of Split Rigidities - I. Jour. Aero. Sci., vol. 18, no. 5, May 1951, pp. 339-349.

12. Bijlaard, P. P.: Analysis of the Elastic and Plastic Stability of Sandwich Plates by the Method of Split Rigidities - II. Jour. Aero. Sci., vol. 18, no. 12, Dec. 1951, pp. 790-796, 829.

13. Bijlaard, P. P., and Fisher, G. P.: Interaction of Column and Local Buckling in Compression Members. NACA TN 2640, 1952.

14. Bijlaard, P. P.: Analysis of the Elastic and Plastic Stability of Sandwich Plates by the Method of Split Rigidities - III. Jour. Aero. Sci. (Readers' Forum), vol. 19, no. 7, July 1952, pp. 502-503.

15. Bijlaard, P. P.: Determination of the Effective Width of Plates With Small Deviations From Flatness by the Method of Split Rigidities. Proc. First U. S. Nat. Cong. of Appl. Mech. (June 1951, Chicago, Ill.), A.S.M.E., 1952, pp. 357-362.

16. Bijlaard, P. P., and Johnston, G. S.: Compressive Buckling of Plates Due to Forced Crippling of Stiffeners. Pts. I and II. S.M.F. Fund Paper No. FF-8, Inst. Aero. Sci., Jan. 1953.

17. Bijlaard, P. P., and Fisher, G. P.: Column Strength of H-Sections and Square Tubes in Postbuckling Range of Component Plates. NACA TN 2994, 1953.

18. Bijlaard, P. P.: Analysis of the Buckling of Stiffened Plates, Having Any Number of Stiffeners. Rep. No. 02-984-013, Bell Aircraft Corp., July 1953.

19. Bijlaard, P. P.: Buckling Under External Pressure of Cylindrical Shells Evenly Stiffened by Rings Only. Rep. No. 02-941-002, Bell Aircraft Corp., May 21, 1952.

20. Bijlaard, P. P.: On the Buckling of Stringer Panels Including Forced Crippling. Jour. Aero. Sci., vol. 22, no. 7, July 1955, pp. 491-501.

21. Schmitt, A. F.: The Buckling Effectiveness of Doubler-Reinforced Sheet. Proc. First Midwestern Conf. on Solid Mech., College of Eng., Univ. of Ill., 1953, pp. 11-13.

22. Plantema, F. J., and DeKock, A. C.: The Elastic Overall Instability of Sandwich Plates With Simply Supported Edges. Rep. S. 346, Nationaal Luchtvaartlaboratorium (Amsterdam), 1949.

23. Plantema, F. J.: Theory and Experiments on the Elastic Overall Instability of Flat Sandwich Plates. Rep. S. 402, Verslagen en Verh., Nationaal Luchtvaartlaboratorium (Amsterdam), 1952.

24. Bijlaard, P. P.: Knikzekerheid van door koppelplaten verbonden profielen (Safety Against Buckling of Built-Up Sections Connected by Batten Plates). De Ingenieur (The Hague, Holland), Nr. 7, Feb. 17, 1933, pp. 31-36.

25. Bleich, Friedrich: Buckling Strength of Metal Structures, First ed., McGraw-Hill Book Co., Inc., 1952.

26. Timoshenko, S.: Theory of Elastic Stability. First ed., McGraw-Hill Book Co., Inc., 1936.

27. Seide, Paul: Shear Buckling of Infinitely Long Simply Supported Metalite Type Sandwich Plates. NACA TN 1910, 1949.

28. Seide, Paul: Compressive Buckling of Flat Rectangular Metalite Type Sandwich Plates With Simply Supported Loaded Edges and Clamped Unloaded Edges (Revised). NACA TN 2637, 1952.

29. Bijlaard, P. P.: Approximative Method of Analysis for Rectangular Reinforced Concrete Plates Under Uniformly Distributed or Hydrostatic Load. Third Cong., Int. Assoc. for Bridge and Structural Eng. (Liège), 1948, pp. 507-517.

30. Timoshenko, S.: Theory of Plates and Shells. McGraw-Hill Book Co., Inc., 1940.

31. Libove, Charles, and Batdorf, S. B.: A General Small-Deflection Theory for Flat Sandwich Plates. NACA Rep. 899, 1948. (Formerly NACA TN 1526.)

32. Seide, Paul: The Stability Under Longitudinal Compression of Flat Symmetric Corrugated-Core Sandwich Plates With Simply Supported Loaded Edges and Simply Supported or Clamped Unloaded Edges. NACA TN 2679, 1952.

33. Bijlaard, P. P.: A Theory of Plastic Buckling With Its Application to Geophysics. Verh. Koninklijke Nederlandsche Akad. Wetenschappen, vol. XLI, no. 5, 1938, pp. 468-480.

34. Bijlaard, P. P.: Theory and Tests on the Plastic Stability of Plates and Shells. Jour. Aero. Sci., vol. 16, no. 9, Sept. 1949, pp. 529-541.

35. Lardy, P.: Sur une méthode nouvelle de résolution du problème des dalles rectangulaires encastrées. Pub. Int. Assoc. for Bridge and Structural Eng. (Zürich), vol. 13, 1953, pp. 197-220.

36. Bijlaard, P. P.: Buckling Stress of Thin Cylindrical Clamped Shells Subject to Hydrostatic Pressure. Jour. Aero. Sci., vol. 21, no. 12, Dec. 1954, pp. 852-853.

37. Strutt, John William: The Theory of Sound. Second ed., vol. I, Dover Pub., 1945, p. 272.

38. Libove, Charles, and Hubka, Ralph E.: Elastic Constants for Corrugated-Core Sandwich Plates. NACA TN 2289, 1951.

39. Krivetsky, A.: Plasticity Parameters and Coefficients for Plates and Shells. Rep. No. 02-984-019, Bell Aircraft Corp., Nov. 10, 1954.

40. Kollbrunner, C. F.: Present Situation in Switzerland With Regard to Experiments on Buckling With Indication of the Buckling Values k. Fifteenth Int. Cong. Steel Information Centers (Brussels), Oct. 1953.

41. Bijlaard, P. P.: Buckling in the Presence of Thermal Stresses. Rep. no. 9054-18-001, Bell Aircraft Corp., Dec. 1954.

42. Winter, G.: Performance of Compression Plates as Parts of Structural Members. Res. Eng. Structures Supp., Academic Press (New York), pp. 179-185, 1949.

43. Mayers, J., and Budiansky, Bernard: Analysis of Behavior of Simply Supported Flat Plates Compressed Beyond the Buckling Load Into the Plastic Range. NACA TN 3368, 1955.

44. Needham, Robert A.: The Ultimate Strength of Aluminum-Alloy Formed Structural Shapes in Compression. Jour. Aero. Sci., vol. 21, no. 4, Apr. 1954, pp. 217-229.

45. Anderson, Roger A., and Anderson, Melvin S.: Correlation of Crippling Strength of Plate Structures With Material Properties. NACA TN 3600, 1956.

46. Botman, M.: De experimentele bepaling van de meedragende breedte van vlakke platen in bet elastische en bet plastische gebied (deel II) (The Experimental Determination of the Effective Width of Flat Plates in the Elastic and Plastic Range (part II)). Rep. S. 438, Nationaal Luchtvaartlaboratorium (Amsterdam), Jan. 1954.

47. Seide, Paul, and Stein, Manuel: Compressive Buckling of Simply Supported Plates With Longitudinal Stiffeners. NACA TN 1825, 1949.

48. Kollbrunner, Curt Friedrich: Das Ausbeulen der auf einseitigen, gleichmässig verteilten Druck beanspruchten Platten im elastischen und plastischen Bereich. Mitt. Inst. Baustatik (Zürich), Nr. 17, 1946.

49. Bijlaard, P. P.: Theory of the Plastic Stability of Thin Plates. Pub. Int. Assoc. for Bridge and Structural Eng. (Zürich), vol. 6, 1940-41, pp. 45-69.

50. Lundquist, Eugene E., Stowell, Elbridge Z., and Schuette, Evan H.: Principles of Moment Distribution Applied to Stability of Structures Composed of Bars and Plates. NACA Rep. 809, 1945. (Supersedes NACA ARR 3K06.)

51. Kroll, W. D.: Tables of Stiffness and Carry-Over Factor for Flat Rectangular Plates Under Compression. NACA ARR 3K27, 1943.

TABLE 1.- COMPARISON OF RESULTS FROM EQUATIONS (46) AND (48)

l, cm	c, cm	n	h, cm	$m = (l_{eq}/r)/(c/r_c)$					
				$\nu = 0$		$\nu = 4 \times 10^{-5}$ cm/kg		$\nu = 30 \times 10^{-5}$ cm/kg	
				Eq. (46)	Eq. (48)	Eq. (46)	Eq. (48)	Eq. (46)	Eq. (48)
260	130	2	16	1.11	1.09	1.45	1.37	1.84	1.80
390	130	3	16	1.27	1.24	1.70	1.63	2.47	2.42
520	130	4	16	1.47	1.43	1.90	1.85	2.94	2.89
520	130	4	24	1.24	1.21	1.51	1.46	2.39	2.33
780	130	6	16	1.92	1.89	2.30	2.26	3.56	3.53
156	78	2	16	1.12	1.09	1.56	1.48	1.89	1.89
390	78	5	16	1.69	1.65	2.30	2.26	3.68	3.66
780	78	10	16	2.94	2.91	3.37	3.34	5.09	5.09

TABLE 2.- VALUES p AND q IN EQUATION (203)

AND $\gamma\varphi$ FROM EQUATIONS (211) AND (221)

n	p	q	$\gamma\varphi$
2	2.27	2.45	0.570
3	2.36	3.58	.616
4	2.37	4.20	.639
∞	2.5	5	.707

TABLE 3.- COMPARISON OF RESULTS FROM EQUATION (224) WITH THOSE FROM REFERENCE 47

n	2	2	3	3	4	4	4	∞	∞	∞	∞
EI/(bN)	5	5	5	0	5	2	0	5	2	5	0
δ	0	0.4	0	0	0	0	0	0	0	0.4	0.4
k_{cr} from eq. (224) . . .	4.15	3.73	4.22	1.235	4.25	2.78	1.13	4.25	2.66	3.59	0.71
k_{cr} from ref. 47	4.20	3.75	4.25	(1.28)	4.25	2.79	1.13	4.25	2.66	3.60	0.71

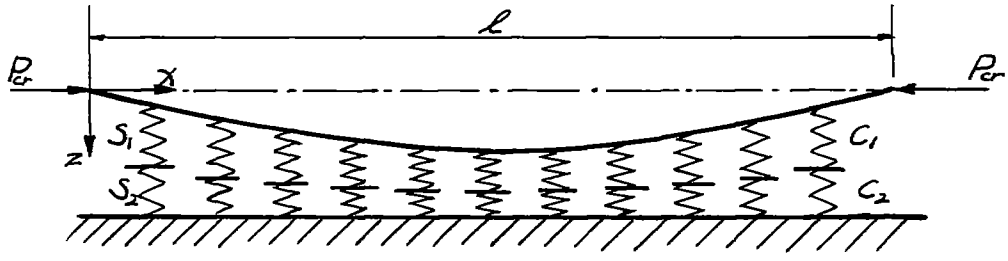

Figure 1.- Replacement of bending and shearing rigidity of sandwich column by equivalent spring systems.

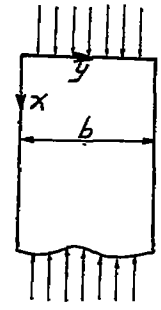

Figure 2.- Long rectangular sandwich plate compressed in X-direction with various boundary conditions at loaded and unloaded edges.

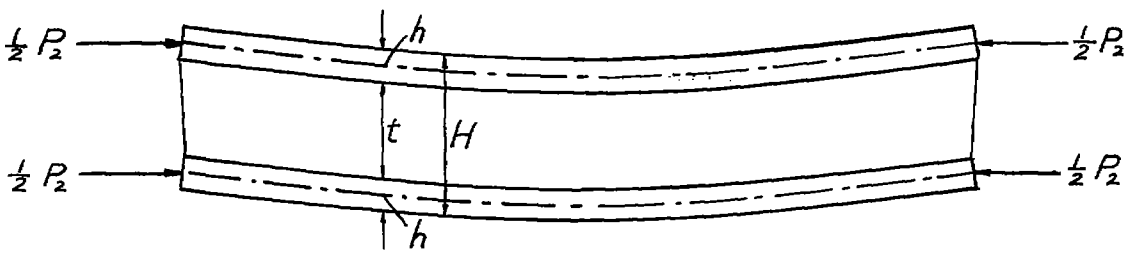

Figure 3.- Longitudinal section of sandwich plate with buckling deflection in case 2 (shear deformation of case only).

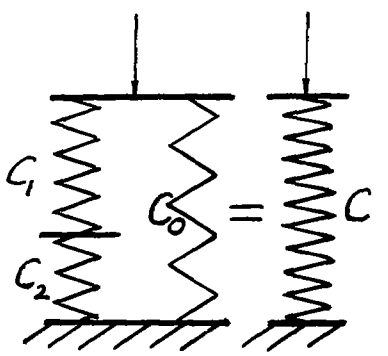

(a) (b)

Figure 4.- Spring systems.

(a) Simply supported case.

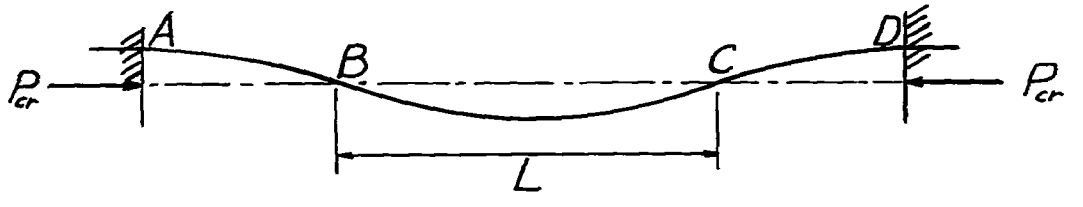

(b) Clamped at both ends.

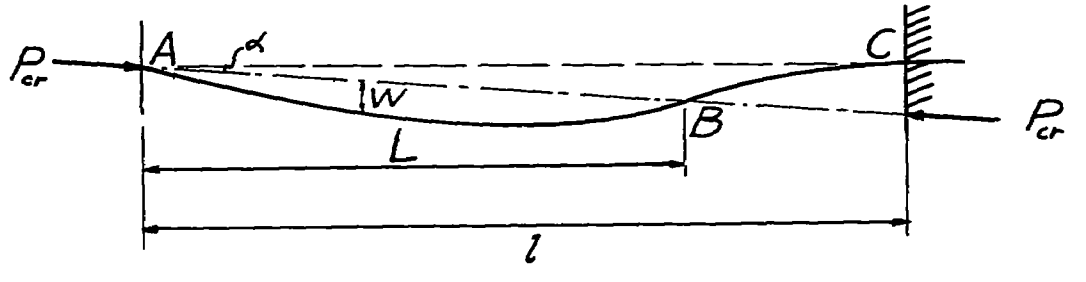

(c) Clamped simply supported case.

Figure 5.- Sandwich columns.

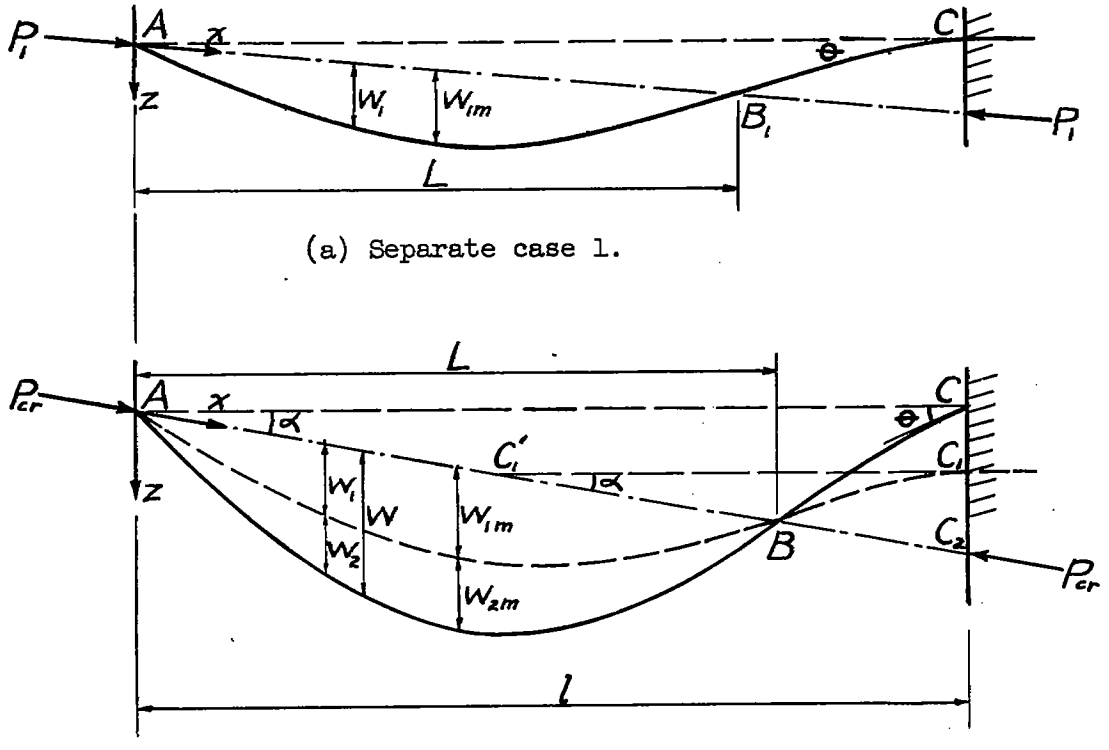

(a) Separate case 1.

(b) Composite case.

Figure 6.- Clamped simply supported sandwich column.

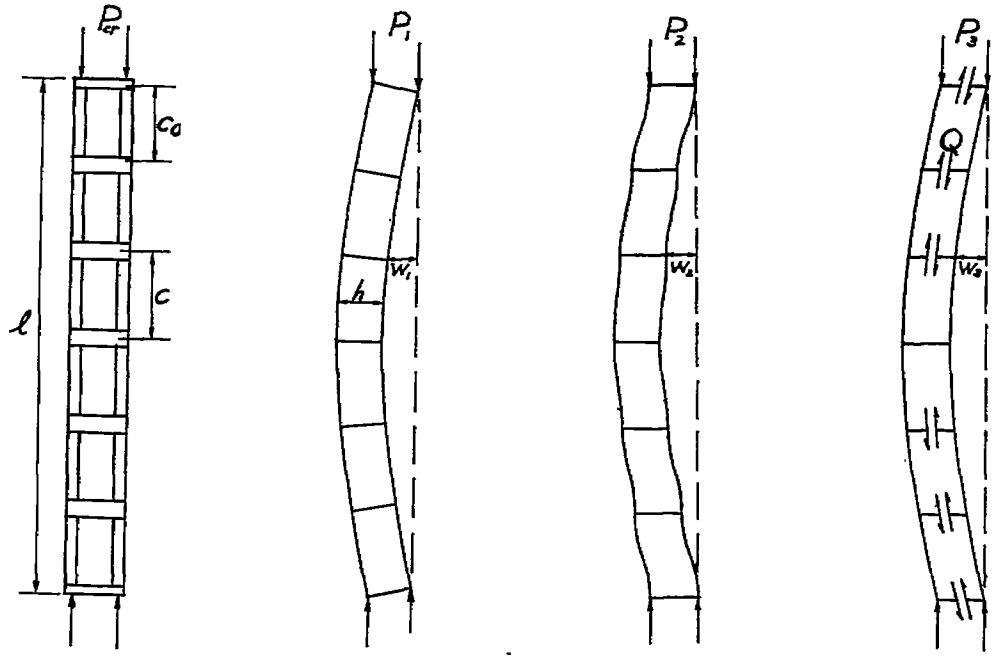

(a) Columns connected by batten plates with equal spacings.

(b) Case 1.

(c) Case 2.

(d) Case 3.

Figure 7.- Columns with batten plates.

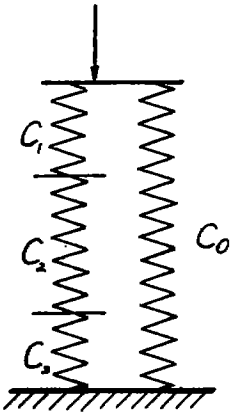

Figure 8.- Equivalent laterally supporting spring system for column with batten plates.

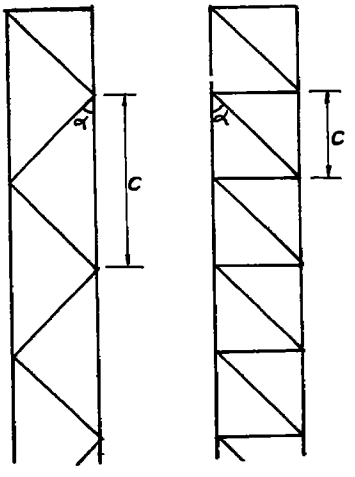

(a) Coupled by diagonals.

(b) Coupled by diagonals and verticals.

Figure 9.- Latticed columns.

2D

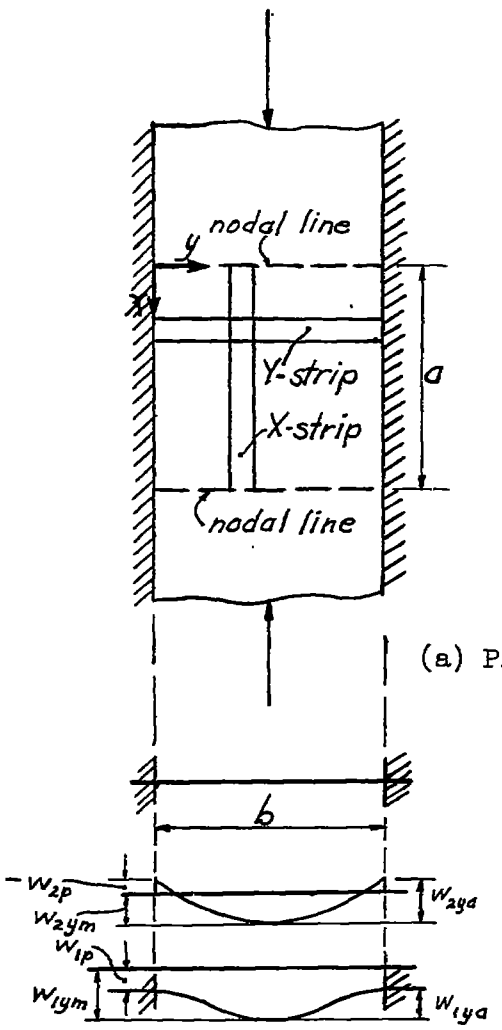

(a) Plan and cross section.

(b) Tentative deflections of Y-strips if constant ratio w_{2m}/w_{1m} is prescribed.

Figure 10.- Long sandwich plate compressed in X-direction and clamped at unloaded edges.

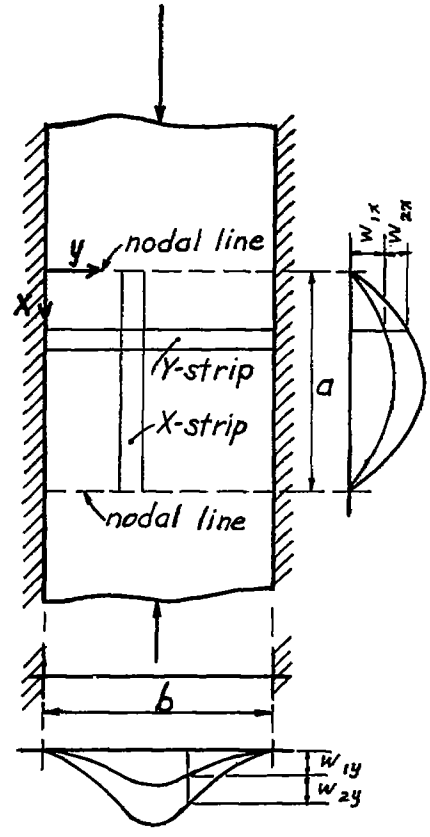

Figure 11.- Long sandwich plate with isotropic faces and an orthotropic core compressed in X-direction with arbitrary boundary conditions at unloaded edges.

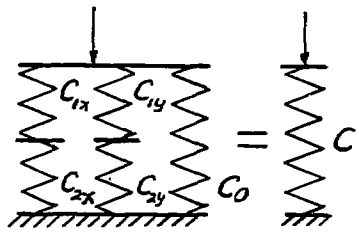

Figure 12.- Equivalent spring systems.

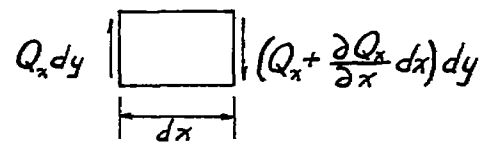

Figure 13.- Restraining forces exerted by X-strip.

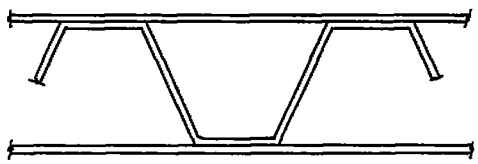

Figure 14.- Cross section of corrugated sandwich plate.

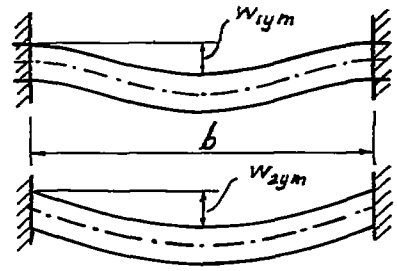

Figure 15.- Deflections of Y-strips for clamped plates.

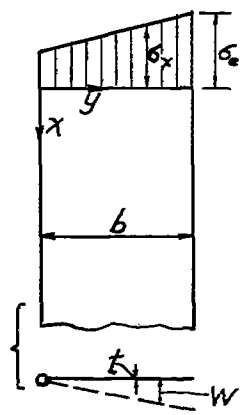

Figure 16.- Buckling of long simply supported flange under linearly distributed stresses that increase with y.

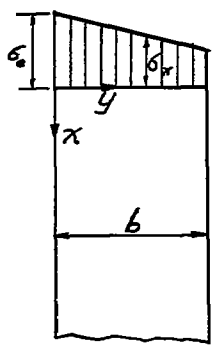

Figure 17.- Buckling of long simply supported flange under linearly distributed stresses that decrease with increasing y.

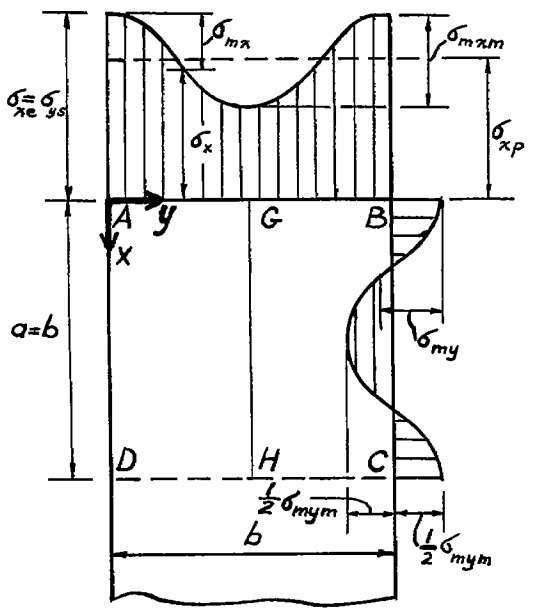

Figure 18.- Distribution of total direct stresses σ_x and σ_y in postbuckling range.

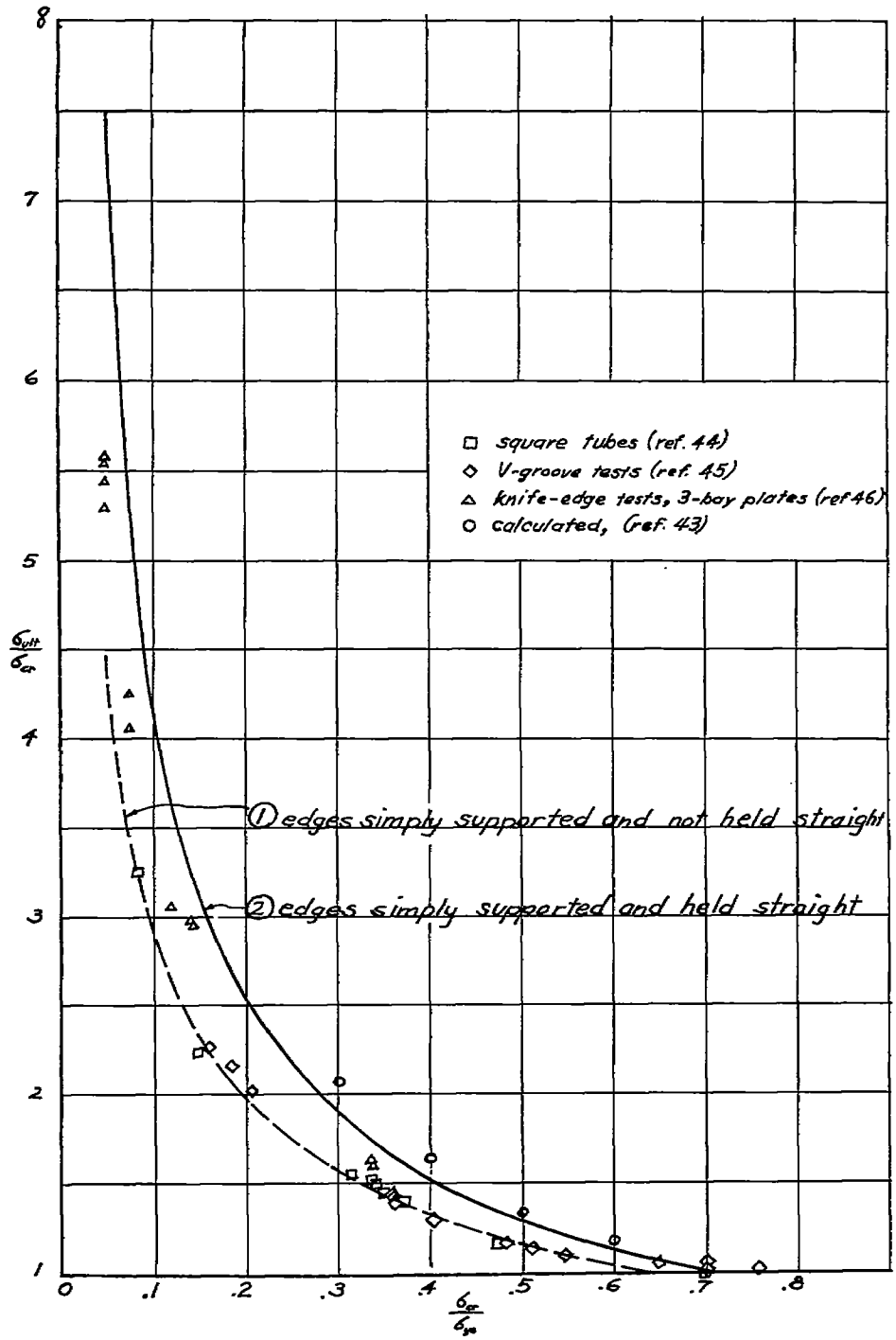

Figure 19.- Plot of σ_{ult}/σ_{cr} as function of σ_{cr}/σ_{ys}.

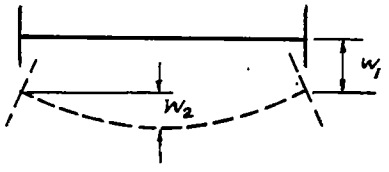

(a) Total deflection.

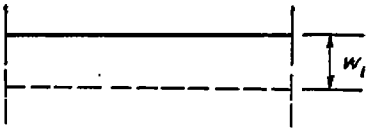

(b) Deflection for case 1.

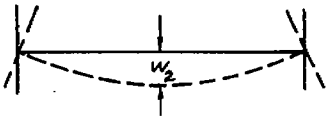

(c) Deflection for case 2.

Figure 20.- Deflection of cross section of I-section.

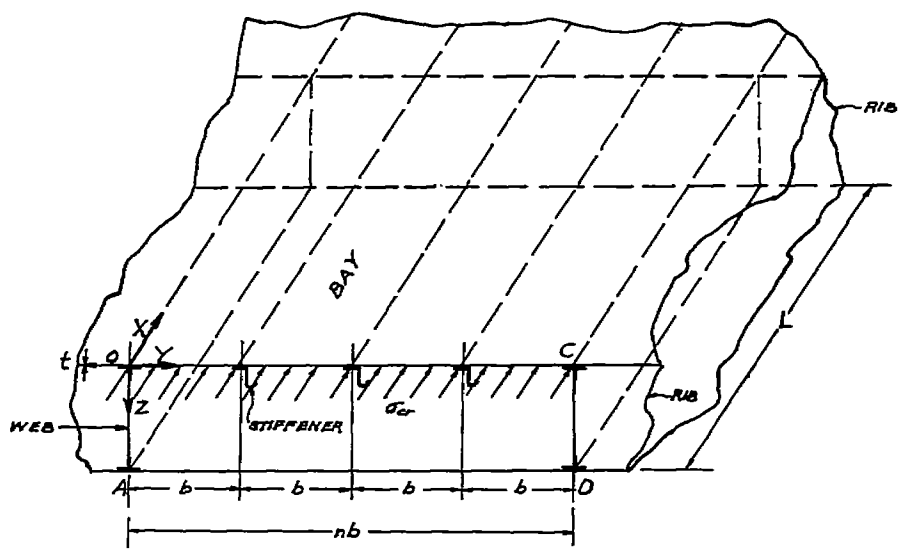

Figure 21.- Stringer panels supported by stiffeners of equal cross section and located at equal distances.

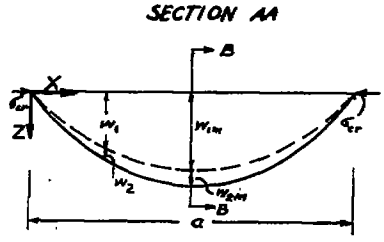

(a) Longitudinal section through center of buckle.

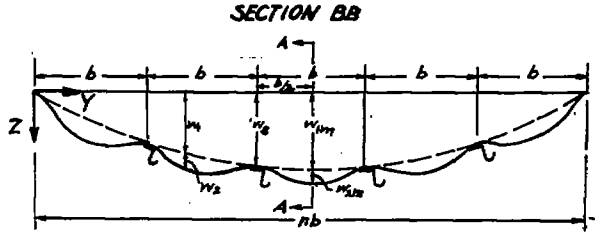

(b) Cross section through center of buckle.

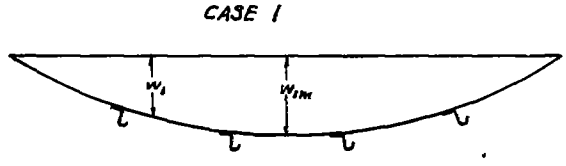

(c) Cross section with deflection in case 1.

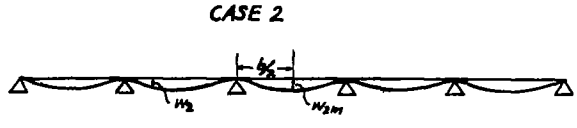

(d) Cross section with deflection in case 2.

Figure 22.- Buckling deflection of stringer panel.

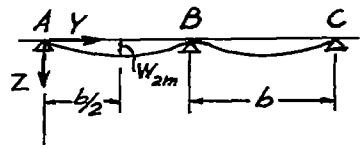

(a) n = 2.

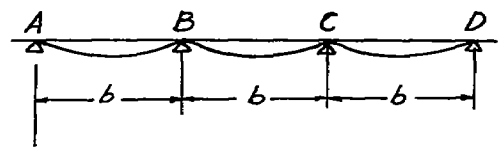

(b) n = 3.

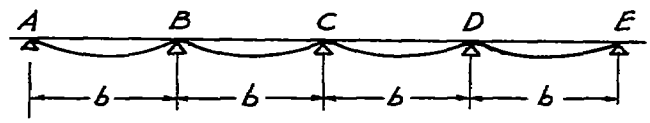

(c) n = 4.

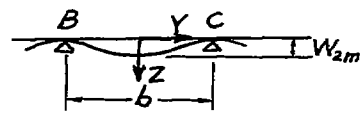

(d) n = ∞.

Figure 23.- Sketches used in computation of p, q, and $\gamma\varphi$.